

Censored and Fair Universal Representations using Generative Adversarial Models

Peter Kairouz* Jiachun Liao* Chong Huang Lalitha Sankar *

Abstract

We present a data-driven framework for learning *censored and fair universal representations* (CFUR) that ensure statistical fairness guarantees for all downstream learning tasks that may not be known *a priori*. Our framework leverages recent advancements in adversarial learning to allow a data holder to learn censored and fair representations that decouple a set of sensitive attributes from the rest of the dataset. The resulting problem of finding the optimal randomizing mechanism with specific fairness/censoring guarantees is formulated as a constrained minimax game between an encoder and an adversary where the constraint ensures a measure of usefulness (utility) of the representation. We show that for appropriately chosen adversarial loss functions, our framework enables defining demographic parity for fair representations and also clarifies the optimal adversarial strategy against strong information-theoretic adversaries. We evaluate the performance of our proposed framework on multi-dimensional Gaussian mixture models and publicly datasets including the UCI Census, GENKI, Human Activity Recognition (HAR), and the UTKFace. Our experimental results show that multiple sensitive features can be effectively censored while ensuring accuracy for several *a priori* unknown downstream tasks. Finally, our results also make precise the tradeoff between censoring and fidelity for the representation as well as the fairness-utility tradeoffs for downstream tasks.

Keywords: Censored Representations, Algorithmic Fairness, Generative Adversarial Networks, Minimax Games, Information-theoretic Guarantees.

1 Introduction

The use of deep learning algorithms for data analytics has recently seen unprecedented success for a variety of problems such as image classification, natural language processing, and prediction of consumer behavior, electricity use, political preferences, to name a few. The success of these algorithms hinges on the availability of large datasets that may include patterns of societal bias and discrimination as well as sensitive personal information. It has been shown that models learned from such datasets can potentially inherit such biases [Ladd, 1998, Pedreshi et al., 2008] as well as glean sensitive features even when such features are not explicitly used during training [Song and Shmatikov, 2019]. As a result, concerns about the fairness, bias, and privacy of learning algorithms has led to a growing body of research focused on both defining meaningful fairness measures and designing learning models with a desired fairness guarantee (see [Mehrabi et al., 2019, Feldman et al., 2015a] for detailed surveys of both measures and approaches) as well as identifying methods to censor or obfuscate sensitive features [Calders and Žliobaitė, 2013].

While the fundamental question of how to formally define algorithmic fairness continues to be open, most algorithmic fairness measures have been motivated by legal systems that evaluate the fairness of a decision-making process using two distinct notions [Barocas and Selbst, 2016]: *disparate treatment* and *disparate impact*. The process of making decisions suffers from disparate treatment if

**.: equal contribution

the decisions are (partly) based on the subject’s sensitive attribute, and it has disparate impact if its outcomes disproportionately hurt (or benefit) people with certain sensitive attribute values. These two legal definitions have led to many distinct interpretations of algorithmic fairness, and therefore, to many quantitative measures. Furthermore, whether fairness should be enforced at a group or individual level has also led to different quantitative definitions (see [Mehrabi et al., 2019, Jung et al., 2019, Lahoti et al., 2019] and the references therein) and two broad approaches: group fairness and individual fairness. Irrespective of the fairness measure, ensuring algorithmic fairness requires processing the data either before (pre-processing), during (in-processing), or after (post-processing) the decision making process.

The bulk of research focused on fair machine learning (ML) has been in ensuring that specific decisions (e.g., classification, regression, ranking) are fair. In a variety of data collection settings, however, the learning tasks may not be known *a priori* or the data may be collected for learning multiple tasks. In this context, instead of designing a fair learning model for a specific task, we propose to learn a model that outputs a censored and fair universal representation (CFUR) of the data at hand. The resulting representation can then be used to learn a variety of task-appropriate models that are information-theoretically guaranteed to be fair. These representations are universal and fair in that the representations can be used for a variety of downstream learning tasks and the fairness guarantees are independent of such tasks. Since fairness assurances for CFURs are achieved via pre-processing the data, a reasonably appropriate measure of fairness is the group fairness measure of demographic parity (DemP) which ensures the same proportion of outcomes to all groups. As an immediate consequence of such pre-processing, the CFUR problem becomes a tradeoff between ensuring sufficient fidelity of the representation to ensure high accuracy on downstream learning tasks while guaranteeing a desired measure of demographic parity.

The key idea of our CFUR approach is that of actively decorrelating the sensitive data from the other features, thereby ensuring that the downstream tasks are learned independent of such sensitive features. As a result, the CFUR model itself serves broader purpose: it can be used to create decorrelated representations for new data (from the same distribution or via transfer learning for other datasets) prior to learning any task on it. One can view this effort as a *censoring* approach, i.e., all sensitive features are not just stripped from the data but its correlation with other features are actively damped to censor/restrict its inference from the representation while ensuring some measure of usefulness of the data.

More generally, when learning data representations, censoring and fairness are very similar in that both can be ensured by perturbing the dataset to decorrelate the sensitive variables from the rest of the dataset. Depending on the context and problem requirement, decorrelating operations can be designed as privacy preserving mechanisms to hide the sensitive variables from inference or as a fairness enforcing algorithm that prevents a machine learning model from discriminating based on the sensitive variables. We now detail our specific contributions to designing fair universal representations via a censoring approach.

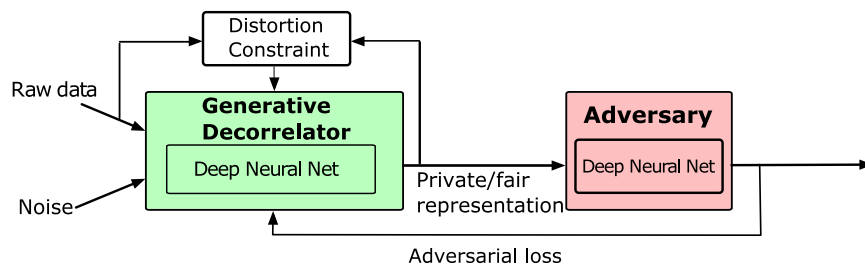


Figure 1: Generative adversarial model for censoring and fairness

1.1 Our Contributions.

There has been a lot of interest recently in using generative models and/or adversarial training methods for both censoring and fairness, and, in particular, to learn fair data representations by censoring sensitive features [Hamm, 2017, Louizos et al., 2016, Edwards and Storkey, 2016, Iwasawa et al., 2017, Xie et al., 2017, Huang et al., 2017, Madras et al., 2018, Zhang et al., 2018, Li et al., 2018, Coavoux et al., 2018, Elazar and Goldberg, 2018, Creager et al., 2019]. Generative adversarial models model the fairness and censoring problem as a *constrained minimax game* between an adversary, intent on learning the sensitive features, and the fair encoder interested in producing a representation that is constrained to ensure high accuracy on a chosen learning task (typically classification). Some approaches listed above also ensure that the representation itself has high fidelity [Edwards and Storkey, 2016] but the focus on all research to-date is primarily on ensuring high classification accuracy for a desired fairness guarantee. More broadly, the bulk of these approaches have three main limitations:

(A) Learn a representation for a specific task, and thus, require the designer to have access to labels from a ML classification task of interest at training time. However, having these labels at training time is not always feasible (for instance, the vast majority of on-device images are not labeled for various ML tasks); furthermore, knowing the task *a priori* is often difficult and it’s desirable to design representations that work well for a variety of downstream ML tasks.

(B) Mostly provide empirical guarantees against *computationally finite adversaries*, i.e., adversaries modeled by a learning model with finitely many parameters and capturing a specific class of hypotheses as well as adversarial action (via the loss function).

(C) Largely run simple experiments on relatively small (often categorical) datasets with limited, if any, visualizations of how the representations restrict sensitive attributes.

Given this, it is natural and important to address the following questions: (i) how can we obtain representations that work well without having any specific learning task in mind at training time, and (ii) how well do the learned representations perform against more powerful adversaries? While using a constrained minimax framework analogous to prior efforts, our work addresses these questions via the following contributions.

1. Our approach addresses (A), the problem of learning a fair representation, by including only one constraint, namely a fidelity (distortion) in the minimax game, to ensure that the representation learned can be useful for a variety of downstream learning tasks. The distortion constraint we impose presents a novel challenge on training GAN-like models under constraints. Until recently, most ML libraries (e.g., PyTorch, TensorFlow) did not allow ML engineers to enforce hard constraints on the optimization problems being solved. We address this by solving the hard constrained optimization problem in these existing ML frameworks using the Penalty and Augmented Lagrange barrier methods. In fact, the recently introduced TensorFlow package [Google, Cotter et al., 2019b] takes precisely this approach to do so.
2. To address question (B) above, we show that our framework (via Theorem 1, Corollary 1, and Proposition 1) recovers an array of (operationally motivated) information-theoretic notions of adversarial learning. In particular, our framework directly captures two key metrics for fairness, namely, demographic parity and equalized odds (when learning representations for a specific classification task) via the choice of the loss function and possible information available during adversarial training. We critically leverage this connection to show that fair and censored representations learned in a data-driven fashion against a finite adversary hold up well when attacked by the game-theoretically optimal adversary. Specifically, this allows us to compare data-driven approaches directly against strong inferential adversaries (e.g., a maximum *a posteriori* probability (MAP) adversary with access to dataset statistics),

particularly for synthetic datasets wherein the optimal encoder for the strongest adversary can be computed.

3. The strong connections we draw between game-theoretic and information theoretic formulations can be of independent interest to machine learning practitioners interested in optimizing empirical information theoretic measures (such as mutual information). Instead of using variational techniques (by optimizing lower/upper bounds on the objective function) [Alemi et al., 2016], our work shows that ML engineers can solve a minimax problem with the oft-used log loss (cross entropy loss). We also introduce a systematic method using mutual-information estimation to certify that the learned representations will perform well against unseen, more complex adversaries. On the fairness front, via the use of log-loss as the adversarial loss function (and hence the fair encoder’s gain function), our framework demonstrates how minimizing mutual information can serve as a proxy for demographic/statistical parity.
4. To showcase the power of our approach, we conduct 3 sets of extensive experiments on a variety of datasets: GENKI [Whitehill and Movellan, 2012], HAR [Anguita et al., 2013], UCI Adult [Kohavi, 1996], and UTKFace [Zhang and Qi, 2017]. For relevant datasets, our visual results show that our data driven training methods succeed at creating high quality representations that increasingly erase the sensitive attributes with decreasing fidelity requirements. Both our theoretical framework and our experiments consider non-binary sensitive attributes and datasets with multiple attributes. Our experimental results show that one can still learn high quality classifiers even when the downstream ML task is not known *a priori*. In particular, we consider the UCI dataset that is often used in fair ML analyses to showcase the advantage of our approach relative to related approaches (for example, by Edwards and Storkey [Edwards and Storkey, 2016], Madras *et al.* [Madras et al., 2018, Creager et al., 2019], and Mitchell *et al.* [Zhang et al., 2018], among others). Moreover, our results straddle a wide range of values for the chosen fairness measure (demographic parity) including perfect fairness, in contrast to the above cited works.

1.2 Related Work

Fair ML is of much interest in practice, and this has led to a growing body of research on defining fairness measures, quantifying rigorous guarantees, and developing data-driven methods to learn fair models [Gutmann and Hyvärinen, 2010, Salimans et al., 2016, Odena, 2016, Luc et al., 2016, Ganin et al., 2016, Hardt et al., 2016, Calmon et al., 2017, 2018, Gupta et al., 2018, Cotter et al., 2019b, Agarwal et al., 2019, Narasimhan et al., 2019, Cotter et al., 2019a, Beutel et al., 2019a,b, Garg et al., 2019, Lewandowski and Spree, 2011, Yang and Stoyanovich, 2017, Zehlike et al., 2017, Biega et al., 2018, Singh and Joachims, 2018, Narasimhan et al., 2019, Beutel et al., 2019a].

A key challenge in algorithmic fairness is that of quantifying disparate impact and treatment; efforts in this direction have led to a variety of measures. Broadly, two distinct approaches have emerged: one approach is that of ensuring statistical or demographic parity by seeking similar outcomes for all groups [Feldman et al., 2015b]. In contrast, the alternative perspective is that of individual fairness which requires treating similar individuals, perceived as such in some measurable space, similarly [Dwork et al., 2012]. Approaches that combine/balance group and individual fairness requirements have also been considered [Calmon et al., 2017, 2018, Kearns et al., 2018, Lahoti et al., 2019]. Fairness has also been quantified in the supervised setting by ensuring equal predictive error rates for all groups [Hardt et al., 2016] or ensuring that outcomes are independent of protected attributes, conditioned on the risk [Chouldechova, 2017]. Yet another compelling approach to fairness has been that of *anti-classification* [Corbett-Davies and Goel, 2018] wherein protected attributes (e.g., race, gender, and their correlates) are not explicitly used to make decisions. This

in turn has led to algorithmic fairness guarantees via censoring [Hamm, 2017, Louizos et al., 2016, Edwards and Storkey, 2016, Iwasawa et al., 2017, Xie et al., 2017, Huang et al., 2017, Madras et al., 2018, Zhang et al., 2018, Li et al., 2018, Coavoux et al., 2018, Elazar and Goldberg, 2018, Creager et al., 2019]. While each approach has its tradeoffs and social costs [Corbett-Davies and Goel, 2018], in this paper we take the approach of censoring to develop fair models that can generate representations for a variety of downstream learning tasks, each of which is assured a desired fairness guarantee.

Fairness guarantees for specific learning tasks can be achieved either via pre-processing, or in-processing, or post-processing the data. In-processing approaches are most commonly used in the supervised setting where the learning objective (e.g., target labels for classification) are known, and have been explored in the context of classification [Dwork et al., 2012, Fish et al., 2016, Zhang et al., 2018, Beutel et al., 2019b, Garg et al., 2019], regression [Agarwal et al., 2019, Narasimhan et al., 2019] and ranking [Lewandowski and Spree, 2011, Yang and Stoyanovich, 2017, Zehlike et al., 2017, Biega et al., 2018, Singh and Joachims, 2018, Beutel et al., 2019a]. In this setting, knowledge of the learning objective/task is required in the training phase and the resulting trained model gives fair results only for the specified learning objective. Therefore, in-processing approaches are not applicable for datasets with limited or no labels. Pre-processing approaches generally produce fair representations of data at hand and post-processing approaches provide fairness by properly altering decision outputs [Calmon et al., 2017, Hajian et al., 2015, McNamara et al., 2017, Louizos et al., 2016]. Both these two approaches do not require the knowledge of learning objectives in the training phase.

Instead of learning a fair model for a specific task, one can alternatively learn fair representations of datasets. Learning fair representations using information-theoretic objective functions and constrained optimization have been proposed in [Calmon et al., 2017, 2018, Ghassami et al., 2018]. However, these approaches, focusing on information-theoretic formulations, require knowledge of the statistics of the datasets. To circumvent the lack of statistical knowledge for real datasets, *data-driven approach* have been considered wherein fair models are learned directly from the data via adversarial models. Adversarial learning models have been developed [Gutmann and Hyvärinen, 2010, Goodfellow et al., 2014, Mirza and Osindero, 2014] and applied to semi-supervised learning [Salimans et al., 2016, Odena, 2016], domain adaptation [Ganin et al., 2016] and segmentation [Luc et al., 2016]. Recently, such methods have also been applied to context-aware censoring and fairness [Edwards and Storkey, 2016, Abadi and Andersen, 2016, Raval et al., 2017, Huang et al., 2017, Tripathy et al., 2017, Beutel et al., 2017, Madras et al., 2018, Zhang et al., 2018].

In contrast to most fair ML approaches that involve generative models [Edwards and Storkey, 2016, Raval et al., 2017, Huang et al., 2017, Beutel et al., 2017, Madras et al., 2018] wherein the training phase explicitly models a downstream classification task, our framework does not require any downstream application as a prior and preserves utility of generated representation by limiting its fidelity relative to original (non-protected) data. Such an approach is also referred to as censoring in the literature.

Censoring has also been proposed as a method to ensure information-theoretic privacy or obfuscation in a variety of contexts where the information to be censored or obfuscated is precisely known. [Hamm, 2017, Huang et al., 2017, Iwasawa et al., 2017, Xie et al., 2017, Tripathy et al., 2017, Li et al., 2018, Coavoux et al., 2018, Moyer et al., 2018, Bertran et al., 2019]. Indeed, while differential privacy is viewed as the gold standard for context-free privacy, for scenarios in which the sensitive features are known *a priori* and need to be obfuscated prior to using the data, context-aware techniques that allow censoring of the sensitive features have emerged as a viable alternative to ensure utility of published data/representation. Our proposed framework is a context-aware approach focused on learning representations that are decorrelated from specified sensitive features while ensuring some measure of fidelity of the representation relative to original data. Censoring

also allows guaranteeing specific measures of fairness for the representation, and in turn, for the downstream classifiers.

1.3 Outline

The remainder of our paper is organized as follows. We formally defined censored and fair representations in Section 2. In Section 3, we formalize our CFUR model and highlight the theoretical guarantees of this approach. In Section 4, we present theoretical results for datasets modeled as multi-dimensional Gaussian mixtures. Finally, we showcase the performance of the CFUR framework on the GENKI, HAR, UCI Adult, and UTKFace datasets in Section 5. All proofs and algorithms are deferred to appendices in the accompanying supplementary materials.

2 Preliminaries

We consider a dataset \mathcal{D} with n entries where each entry is denoted as (S, X, Y) where $S \in \mathcal{S}$ is a collection of sensitive features, $X \in \mathcal{X}$ is a collection of non-sensitive features, and $Y \in \mathcal{Y}$ is an a priori unknown collection of target (non-sensitive) features to be learned. Let $\hat{Y} \in \mathcal{Y}$ be a prediction of Y . We note that S and Y can be a collection of features or labels (e.g., S can be gender, race, or sexual orientation, while Y could be age, facial expression, etc.); for ease of writing, we use the term variable to denote both single and multiple features/labels. Instances of X , S , and Y are denoted by x , s and y , respectively. We assume that each entry (X, S, Y) is independent and identically distributed (i.i.d.) according to $P(X, S, Y)$.

Recent results on fairness in learning applications guarantees that for a specific target variable, the prediction of a machine learning model is accurate with respect to (*w.r.t.*) the target variable but unbiased *w.r.t.* a sensitive variable. While more than two dozen measures for fairness have been proposed, the three oft-used fairness measures are demographic parity, equalized odds, and equality of opportunity. Demographic parity ensures complete independence between the prediction of the target variable and sensitive variable, and thus, this notion of fairness favors utility the least, especially when the target and sensitive variables are correlated [Hardt et al., 2016]. Equalized odds enforces this independence conditioned on the target variable thereby ensuring equal rates for true and false positives (wherein the target variable is binary) for all demographics. Equal opportunity ensures equalized odds for the true positive case alone [Hardt et al., 2016].

For the sake of completeness, we review these definitions briefly. We note that these definitions are often aimed at sensitive (S) and target (Y) features that are binary, and in reviewing these definitions below, we make this assumption too. However, we note that these definitions can be generalized to the non-binary setting; indeed, our own generalizations of these definitions as applied to representation setting do not make such an assumption.

Definition 1 ([Hardt et al., 2016]) *A predictor $f(S, X) = \hat{Y}$ satisfies*

- *demographic parity w.r.t. the sensitive variable S , if \hat{Y} and S are independent, i.e.,*

$$\Pr(\hat{Y} = 1|S = 1) = \Pr(\hat{Y} = 1|S = 0) \tag{1}$$

- *equalized odds w.r.t. the sensitive variable S and target variable Y , if \hat{Y} and S are independent conditional on Y , i.e.,*

$$\Pr(\hat{Y} = 1|S = 1, Y = y) = \Pr(\hat{Y} = 1|S = 0, Y = y), \quad y \in \{0, 1\} \tag{2}$$

- equality of opportunity w.r.t. the sensitive variable S and target variable Y , if \hat{Y} and S are independent conditional on $Y = 1$, i.e.,

$$\Pr(\hat{Y} = 1|S = 1, Y = 1) = \Pr(\hat{Y} = 1|S = 0, Y = 1). \quad (3)$$

We begin by first defining the notions of censoring and fairness for representations. In particular, as discussed thus far, in the censoring context, our goal is to introduce a definition that ensures that the censored representation limits leakage of sensitive variables from adversaries that can potentially *learn* it from the released data. It is crucial to note that censoring will in general not give the kind of strong privacy guarantees provided by differential privacy but can be relevant for some applications where releasing a representation is crucial.

Definition 2 (Censored Representations) *A representation X_r of X is censored w.r.t. the sensitive variable S against a learning adversary $h(\cdot)$, whose performance is evaluated via a loss function $\ell(h(X_r), S)$, if for an optimal adversarial strategy $h_g^* = \operatorname{argmin}_h \mathbb{E}[\ell(h(g(X)), S)]$ corresponding to any (randomized) function $g(X)$*

$$\mathbb{E}[\ell(h_g^*(g(X)), S)] \leq \mathbb{E}[\ell(h_{g_r}^*(X_r), S)], \quad (4)$$

where $X_r = g_r(X)$ and the expectation is over h , g (or g_r), X , and S .

To motivate the generation of fair representations, we now extend the definition of demographic parity for representations. Indeed it is known that fair representations can be used to ensure fair classification (see, for example, [Hardt et al., 2016]). We formally define fair representation and prove that such representations ensure fair classification.

Definition 3 (Demographically Fair Representations) *Let \mathcal{X}_r and \mathcal{S} be the supports of X_r and S , respectively. A representation X_r of X satisfies demographic parity w.r.t. the sensitive variable S if X_r and S are independent, i.e., for any $x_r \in \mathcal{X}_r$ and $s, s' \in \mathcal{S}$,*

$$\Pr(X_r = x_r|S = s) = \Pr(X_r = x_r|S = s'). \quad (5)$$

Given this definition, we now prove that a fair representation in the sense of demographic parity will guarantee that any downstream learning algorithm making use of the fair representation is fair (in the sense of demographic parity) w.r.t. the sensitive label S .

Theorem 1 (Fair Learning via Fair Representation) *Given a dataset consisting of sensitive, non-sensitive, and target variables (S, X, Y) , respectively, if a fair representation $X_r = g(X)$ satisfies demographic parity w.r.t. S , then any learning algorithm $f : \mathcal{X}_r \rightarrow \mathcal{Y}$ satisfies demographic parity w.r.t. S .*

The proof of Theorem 1 is basically depending on the data-processing inequality of mutual information and the details are in Appendix A.

Remark 1 *Note that the definitions of equalized odds and equality of opportunity in Def. 1 explicitly involve a downstream learning application, and therefore, the design of a fair representation needs to include a classifier explicitly. In contrast to the universal representation setting considered here, such targeted representations and the ensuing fair classifiers provide guarantees only for those targeted Y features. In this limited context, however, one can still define a representation X_r as ensuring equalized odds (w.r.t. to S) in classifying Y if the predicted output learned from X_r , i.e., $\hat{Y}(X_r)$, is independent of S conditioned on Y .*

One simple approach to obtain a fair/censored representation X_r is by choosing $X_r = N$ where N is a random variable independent of X and S . However, such an X_r has no downstream utility (quantified, for example, via downstream task accuracy). More generally, the design of X_r has to ensure utility, and thus, there is a tradeoff between guaranteeing fairness/censoring and assuring a desired level of utility. The CFUR framework enables quantifying these tradeoffs formally as described in the next section.

3 Censored and Fair Universal Representations (CFUR) via Generative Adversarial Models

Formally, the CFUR model consists of two components, an encoder and an adversary as shown in Fig. 1. The goal of the encoder $g : \mathcal{X} \times \mathcal{S} \rightarrow \mathcal{X}_r$ is to actively decorrelate S from X while that of the adversary $h : \mathcal{X}_r \rightarrow \mathcal{S}$ is to infer S . Thus, in general, $g(X, S)$ is a randomized mapping that outputs a representation $X_r = g(X, S)$. Note that the design of $g(\cdot)$ depends on both X and S ; however, we note that S may not necessarily be an input to the encoder though it will always affect the design of $g(\cdot)$ via the adversarial training process. In contrast, the role of the adversary is captured via $h(X_r)$, the adversarial decision rule (classifier) in inferring the sensitive variable S as $\hat{S} = h(g(X))$ from the representation $g(X, S)$. In general, the hypothesis h can be a *hard decision rule* under which $h(g(X))$ is a direct estimate of S or a *soft decision rule* under which $h(g(X)) = P_h(\cdot|g(X))$ is a distribution over \mathcal{S} .

To quantify the adversary’s performance, we use a loss function $\ell(h(g(X = x)), S = s)$ defined for every pair (x, s) . Thus, the adversary’s expected loss *w.r.t.* X and S is $L(h, g) \triangleq \mathbb{E}[\ell(h(g(X)), S)]$, where the expectation is taken over $P(X, S)$ and the randomness in g and h .

Intuitively, the generative (since it randomizes to decorrelate) encoder would like to minimize the adversary’s ability to learn S reliably from X_r . This can be trivially achieved by releasing an X_r independent of X . However, such an approach provides no utility for data analysts who want to learn non-sensitive variables Y from X_r . To overcome this issue, we capture the loss incurred by perturbing the original data via a distortion function $d(x_r, x)$, which measures how far the original data $X = x$ is from the processed data $X_r = x_r$. Ensuring statistical utility in turn requires constraining the average distortion $\mathbb{E}[d(g(X), X)]$ where the expectation is taken over $P(X, S)$ and the randomness in g .

3.1 CFUR: Framework and Theoretical Results

To publish a censored and fair representation X_r , the data curator wishes to learn an encoder g that guarantees both censoring/fairness (in the sense that it is difficult for the adversary to learn S from X_r) as well as utility (in the sense that it does not distort the original data too much). In contrast, for a fixed encoder g , the adversary would like to find a (potentially randomized) function h that minimizes its expected loss, which is equivalent to maximizing the negative of the expected loss. This leads to a constrained minimax game between the encoder and the adversary given by

$$\min_{g(\cdot)} \max_{h(\cdot)} - \mathbb{E}[\ell(h(g(X)); S)], \tag{6a}$$

$$s.t. \quad \mathbb{E}[d(g(X), X)] \leq D. \tag{6b}$$

where the constant $D \geq 0$ determines the allowable distortion of the representation and the expectation is taken over $P(X, S)$ and the randomness in g and h . Note that if needed, the sensitive variable S can be used by the encoder g to generate the representation.

	Loss function $\ell(h(g(X)), s)$	Optimal adversarial strategy h^*	Adversary type
Squared loss	$(h(g(X)) - S)^2$	$\mathbb{E}[S g(X)]$	MMSE adversary
0-1 loss	$\begin{cases} 0 & \text{if } h(g(X)) = S \\ 1 & \text{otherwise} \end{cases}$	$\operatorname{argmax}_{s \in \mathcal{S}} P(s g(X))$	MAP adversary
Log-loss	$\log \frac{1}{P_h(s g(X))}$	$P(s g(X))$	Belief refining adversary
α -loss	$\frac{\alpha}{\alpha-1} \left(1 - P_h(s g(X))^{1-\frac{1}{\alpha}}\right)$	$\frac{P(s g(X))^\alpha}{\sum_{s \in \mathcal{S}} P(s g(X))^\alpha}$	Generalized belief refining adversary

Table 1: The adversaries captured by the CFUR framework by using various loss functions

Theorem 2 *For sufficiently large distortion bound D , the constrained minimax optimization in (6) generates a universal representation X_r that is censored w.r.t. to S .*

Our CFUR framework places no restrictions on the adversary. Indeed, different loss functions and decision rules lead to different adversarial models (see Table 1). The versatility of the CFUR framework to a large class of (inferring) adversarial models is captured by using the recently introduced tunable loss function– α -loss for $\alpha \in [1, \infty]$ [Liao et al., 2018]:

$$\ell_\alpha(h(g(X)), s) = \lim_{\alpha' \rightarrow \alpha} \frac{\alpha'}{\alpha' - 1} \left(1 - P_h(s|g(X))^{\frac{\alpha'-1}{\alpha'}}\right). \quad (7)$$

The authors in [Liao et al., 2018] show that by tuning the parameter $\alpha \in [1, \infty]$, α -loss captures a variety of information-theoretic adversaries ranging from a hard-decision adversary (for $\alpha = \infty$) via the 0-1 loss function $\ell(h(g(X)), s) = \mathbb{I}_{h(g(X)) \neq s}^1$ to a soft-decision adversary (for $\alpha = 1$) via the log-loss function $\ell(h(g(X)), s) = -\log P_h(s|g(X))$. For any given encoder $g(\cdot)$, the following proposition (and the last row of Table 1) presents the optimal adversarial strategy in term of α -loss.

Proposition 1 *Under α -loss, the optimal adversary decision rule that minimizes the expected loss is a ‘ α -tilted’ conditional distribution $P_h^*(s|g(X)) = \frac{P(s|g(X))^\alpha}{\sum_{s \in \mathcal{S}} P(s|g(X))^\alpha}$. Specifically, for $\alpha = 1$ and $\alpha = \infty$, the optimal adversarial strategies reduce to those for log-loss and 0-1 loss, i.e., the true conditional distribution and the maximal a posteriori (MAP) estimation, respectively. In addition, the optimization in (6) reduces to $\min_{g(\cdot)} -H_\alpha^A(S|g(X))$, where $H_\alpha^A(\cdot|\cdot)$ is the Arimoto conditional entropy.*

Referring to the result in Proposition 1, if the adversary uses 0-1 loss, the objective of the mini-max problem in (6) simplifies to $\min_{g(\cdot)} \max_{s \in \mathcal{S}} P(s, g(X)) - 1 = -1 + \min_{g(\cdot)} P_c(S|g(X))$ where the expression $P_c(S|g(X))$ is the probability of correctly guessing of S given $g(X)$ [Asoodeh et al., 2018]; and if the adversary uses log-loss, the objective of the mini-max problem in (6) simplifies to $\min_{g(\cdot)} -H(S|g(X)) = \min_{g(\cdot)} I(g(X), S)$ for any fixed prior distribution of S where $I(g(X), S)$ is the mutual information (MI) between $g(X)$ and S . Both objective functions $P_c(S|g(X))$ and $I(g(X), S)$ can be used as a proxy of demographic parity since their minimal values can only be obtained when S and $g(X)$ are independent. This holds for the series of α -loss for $\alpha \in [1, \infty]$ and leads to the following theorem.

Theorem 3 *Under α -loss (including log-loss and 0-1 loss), the CFUR framework enforces fairness subject to the distortion constraint. As the distortion increases, the ensuing fairness guarantee approaches ideal demographic parity.*

¹Note that for $\alpha = \infty$, α -loss reduces to probability of error, for which the optimal adversarial strategy that minimizes the expected loss is the *maximal a posteriori* (MAP) estimation and the resulting probability of error is 0-1 loss.

The proofs of Theorem 2, Proposition 1, and Theorem 3 are presented in Appendix B. Many notions of fairness rely on computing probabilities to ensure independence of sensitive and target variables that are not easy to optimize in a data-driven fashion. In Theorem 3, we propose α -loss (including log-loss modeled in practice via cross-entropy) in the CFUR framework as a proxy for enforcing fairness.

A predominant approach in the literature in the context of representations and fairness is to explicitly include the intended classification task, i.e., design representations for a specific learning task with demographic parity guarantees [Madras et al., 2018, Edwards and Storkey, 2016]. Our CFUR formulation can be extended to include this special case. As one may expect, this requires including an additional constraint to ensure high accuracy in learning Y thereby specializing (6) to obtain the following minimax game:

$$\min_{g'(\cdot), f(\cdot)} \max_{h(\cdot)} - \mathbb{E}[\ell(h(g'(X))); S] + \lambda \mathbb{E}[\ell'(f(g'(X)), Y)], \quad (8a)$$

$$s.t. \quad \mathbb{E}[d(g'(X), X)] \leq D, \quad (8b)$$

where $f(\cdot)$ be a classifier for a target feature Y , $\lambda > 0$, and $g'(\cdot)$ and $h(\cdot)$ are the encoder and the adversarial classifier, respectively, as in (6). Note that the loss functions $\ell(\cdot)$ and $\ell'(\cdot)$ can be different. The setup in (8) involves an additional constraint ensuring fair classification and is thus, a more constrained optimization than the CFUR framework; in fact, the CFUR is obtained by setting $\lambda = 0$. However, this method even while generating intermediate representations, is primarily intended to design demographically fair classifiers, and therefore, requires knowing the intended learning tasks of some target features. In contrast, via our CFUR framework, we generate demographic parity-based fair representations that in turn allow guaranteeing the same type of fairness to all downstream tasks involving any subset of target features.

One can also design fair classifiers directly without intermediate representations; furthermore, such classifiers can be designed with either demographic parity or equalized odds guarantees. Indeed, with $\lambda = 0$ in (8), we directly obtain the setup for demographically fair classifiers. We now show that our CFUR framework also subsumes the problem of designing predictors/classifiers under equality of opportunity fairness guarantees. Let $\hat{Y} = \tilde{g}(S, X)$ be a predictor/classifier for the targeted variable Y . Note that the $\tilde{g}(\cdot)$ generally depends on both X and S but the dependence on S can be implicit for scenarios where the sensitive information S is not directly available. Let h be a decision rule used by the adversary to infer the sensitive variable S as $\hat{S} = h(\tilde{g}(S, X), Y)$ from the true targeted variable Y and the soft information of the predictor $\tilde{g}(S, X) = P_{\hat{Y}|X, S}$. Analogous to (6), the design of a fair predictor/classifier can be formulated as

$$\min_{\tilde{g}(\cdot)} \max_{h(\cdot)} - \mathbb{E}[\ell(h(\tilde{g}(S, X), Y), S)], \quad (9a)$$

$$s.t. \quad \mathbb{E}[\ell(\tilde{g}(S, X), Y)] \leq L. \quad (9b)$$

Proposition 2 *Under α -loss (incorporating both log-loss and 0-1 loss), the CFUR formulation in (9) enforces fairness subject to the expected loss constraint. As the loss increases, the ensuing fairness guarantee approaches ideal equalized odd of \tilde{g} respect to the sensitive variable S and the targeted variable Y .*

The proof of Proposition 2 is in Appendix B.4. Note that the formulation in (9) can also be used to generate a fair predictor or classifier in term of demographic parity or equality of opportunity. For demographic parity, the adversary will only have $\tilde{g}(S, X)$ as the input; on the other hand, for equalized odds, the adversary will have both $\tilde{g}(S, X)$ and Y as inputs. Finally, for equality of opportunity, the adversary requires access to $\tilde{g}(S, X)$ and only the $Y = 1$ class.

3.2 Data-driven CFUR

Thus far, we have focused on a setting where the data holder has access to $P(X, S)$. When $P(X, S)$ is known, the data holder can simply solve the constrained minimax optimization problem in (6) (game-theoretic version of the CFUR formulation) to obtain an encoding/decorrelation scheme that would perform best against a chosen type of adversary. In the absence of $P(X, S)$, we propose a data-driven version of the CFUR formulation that allows the data holder to learn decorrelation schemes directly from a dataset $\mathcal{D} = \{(x_{(i)}, s_{(i)})\}_{i=1}^n$. Under the data-driven version of the CFUR formulation, we represent the decorrelation scheme via a generative model $g(X; \theta_p)$ parameterized by θ_p . This generative model takes X as input and outputs X_r . In the training phase, the data holder learns the optimal parameters θ_p by competing against a *computational adversary*: a classifier modeled by a neural network $h(g(X; \theta_p); \theta_a)$ parameterized by θ_a . In the evaluation phase, the performance of the learned decorrelation scheme can be tested under a strong adversary that is computationally unbounded and has access to dataset statistics. We follow this procedure in the next section.

In theory, the functions h and g can be arbitrary. However, in practice, we need to restrict them to a rich hypothesis class. Figure 1 shows an example of the CFUR model in which the generative decorrelator and adversary are modeled as deep neural networks. For a fixed h and g , if S is binary and the log-loss is used, we can quantify the adversary’s *empirical loss* using cross entropy

$$L_n(\theta_p, \theta_a) = -\frac{1}{n} \sum_{i=1}^n s_{(i)} \log h(g(x_{(i)}; \theta_p); \theta_a) + (1 - s_{(i)}) \log(1 - h(g(x_{(i)}; \theta_p); \theta_a)). \quad (10)$$

It is easy to generalize cross entropy to the multi-class case using the softmax function. The optimal model parameters are the solutions to

$$\min_{\theta_p} \max_{\theta_a} -L_n(\theta_p, \theta_a), \quad (11a)$$

$$\text{s.t.} \quad \frac{1}{n} \sum_{i=1}^n d(g(x_{(i)}; \theta_p), x_{(i)}) \leq D \quad (11b)$$

The minimax optimization in (11a) is a two-player non-cooperative game between the generative decorrelator and the adversary with strategies θ_p and θ_a , respectively. In practice, we can learn the equilibrium of the game using an iterative algorithm (see Algorithm 1 in Appendix C). We first maximize the negative of the adversary’s loss function in the inner loop to compute the parameters of h for a fixed g . Then, we minimize the decorrelator’s loss function, which is modeled as the negative of the adversary’s loss function, to compute the parameters of g for a fixed h . Observe that the distortion constraint in (11a) makes our minimax problem different from what is extensively studied in previous works. To incorporate the distortion constraint, we use the *penalty method* [Lillo et al., 1993] to replace the constrained optimization problem by adding a penalty to the objective function. The penalty consists of a penalty parameter ρ_t multiplied by a measure of violation of the constraint at the t^{th} iteration. The constrained optimization problem of the generative decorrelator can be approximated by a series of unconstrained optimization problems with the loss function $L_n(\theta_p, \theta_a) + \rho_t (\max\{0, \frac{1}{n} \sum_{i=1}^n d(g(x_{(i)}; \theta_p), x_{(i)}) - D\})^2$, where ρ_t is a penalty coefficient increases with the number of iterations t . The algorithm and the penalty method are detailed in Appendix C.

In the following sections, we detail our results for both synthetic multi-dimensional Gaussian mixture data as well as publicly available datasets including the GENKI, UCI-Adult, Human Activity Recognition (HAR), and the UTKFace datasets. All code is available via github at [Kairouz et al.].

4 CFUR for Gaussian Mixture Models

In this section, we focus on a setting where $S \in \{0, 1\}$ and X is an m -dimensional Gaussian mixture random vector whose mean is dependent on S . Let $P(S = 1) = q$. Let $X|S = 0 \sim \mathcal{N}(-\mu, \Sigma)$ and $X|S = 1 \sim \mathcal{N}(\mu, \Sigma)$, where $\mu = (\mu_1, \dots, \mu_m)$, and without loss of generality, we assume that $X|S = 0$ and $X|S = 1$ have the same covariance Σ .

We consider a MAP adversary who has access to $P(X, S)$ and the censoring mechanism. The encoder's goal is to sanitize X in a way that minimizes the adversary's probability of correctly inferring S from X_r . In order to have a tractable model for the encoder, we mainly focus on linear (precisely affine) representation $X_r = g(X) = X + Z + \beta$, where Z is an independently generated noise vector. This linear representation enables controlling both the mean and covariance of the privatized data. To quantify utility of the privatized data, we use the ℓ_2 distance between X and X_r as a distortion measure to obtain a distortion constraint $\mathbb{E}_{X, X_r} \|X - X_r\|^2 \leq D$.

4.1 Game-Theoretical Approach

Consider the setup where both the encoder and the adversary have access to $P(X, S)$. Further, let Z be a zero-mean multi-dimensional Gaussian random vector. Although other distributions can be considered, we choose additive Gaussian noise for tractability reasons.

Without loss of generality, we assume that $\beta = (\beta_1, \dots, \beta_m)$ is a constant parameter vector and $Z \sim \mathcal{N}(0, \Sigma_p)$. Following similar analysis in Gallager [2013], we can show that the adversary's probability of detection is given by

$$P_d^{(G)} = qQ\left(-\frac{\alpha}{2} + \frac{1}{\alpha} \ln\left(\frac{1-q}{q}\right)\right) + (1-q)Q\left(-\frac{\alpha}{2} - \frac{1}{\alpha} \ln\left(\frac{1-q}{q}\right)\right), \quad (12)$$

where $\alpha = \sqrt{(2\mu)^T(\Sigma + \Sigma_p)^{-1}2\mu}$. Furthermore, since $\mathbb{E}_{X, X_r}[d(X_r, X)] = \mathbb{E}_{X, X_r}\|X - X_r\|^2 = \mathbb{E}\|Z + \beta\|^2 = \|\beta\|^2 + \text{tr}(\Sigma_p)$, the distortion constraint implies that $\|\beta\|^2 + \text{tr}(\Sigma_p) \leq D$. To make the problem more tractable, we assume both X and Z are independent multi-dimensional Gaussian random vectors with diagonal covariance matrices.

Theorem 4 *Consider the representation given by $g(X) = X + Z + \beta$, where $X|S$ and Z are multi-dimensional Gaussian random vectors with diagonal covariance matrices Σ and Σ_p . Let $\{\sigma_1^2, \dots, \sigma_m^2\}$ and $\{\sigma_{p_1}^2, \dots, \sigma_{p_m}^2\}$ be the diagonal entries of Σ and Σ_p , respectively. The parameters of the minimax optimal censoring mechanism are*

$$\beta_i^* = 0, \quad \sigma_{p_i}^{*2} = \left(\frac{|\mu_i|}{\sqrt{\lambda_0^*}} - \sigma_i^2, 0\right)^+, \quad \forall i = \{1, 2, \dots, m\},$$

where λ_0^* is chosen such that $\sum_{i=1}^m \left(\frac{|\mu_i|}{\sqrt{\lambda_0^*}} - \sigma_i^2\right)^+ = D$. For this optimal mechanism, the accuracy of

the MAP adversary is given by (12) with $\alpha = 2 \sqrt{\sum_{i=1}^m \frac{\mu_i^2}{\sigma_i^2 + \left(\frac{|\mu_i|}{\sqrt{\lambda_0^*}} - \sigma_i^2\right)^+}}$.

The proof of Theorem 4 is provided in Appendix C.1. We observe that when σ_i^2 is greater than some threshold $\frac{|\mu_i|}{\sqrt{\lambda_0^*}}$, no noise is added to the data on this dimension due to the high variance.

When σ_i^2 is smaller than $\frac{|\mu_i|}{\sqrt{\lambda_0^*}}$, the amount of noise added to this dimension is proportional to $|\mu_i|$; this is intuitive since a large $|\mu_i|$ indicates the two conditionally Gaussian distributions are further away on this dimension, and thus, distinguishable. Thus, more noise needs to be added in order to reduce the MAP adversary's inference accuracy.

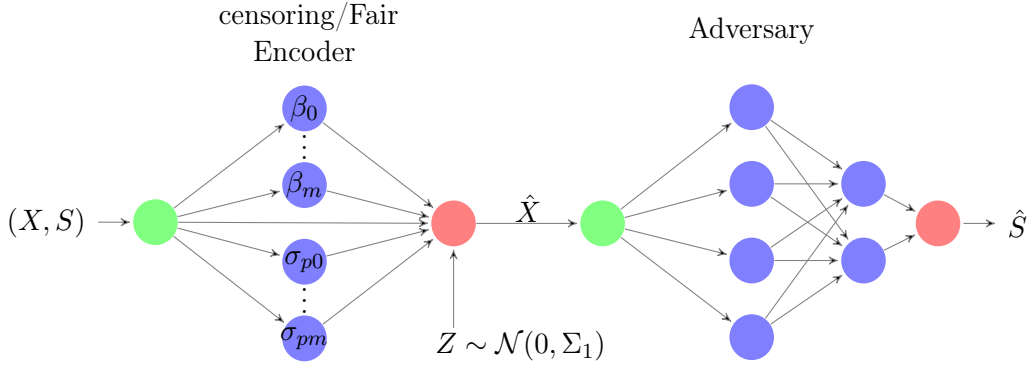


Figure 2: Neural network structure of the linear CFUR for Gaussian mixture data

4.2 Data-driven Approach

For the data-driven linear representation generated from the CFUR framework, we assume the encoder only has access to the dataset \mathcal{D} with n data samples but not the actual distribution of (X, S) . Computing the optimal censoring mechanism becomes a learning problem. In the training phase, the data holder learns the parameters of the CFUR model by competing against a computational adversary modeled by a multi-layer neural network. When convergence is reached, we evaluate the performance of the learned mechanism by comparing with the one obtained from the game-theoretic approach. To quantify the performance of the learned representation, we compute the accuracy of inferring S under a strong MAP adversary that has access to both the joint distribution of (X, S) and the censoring mechanism.

Since the sensitive variable S is binary, we measure the training loss of the adversary network by the empirical log-loss function

$$L_n(\theta_p, \theta_a) = -\frac{1}{n} \sum_{i=1}^n s_{(i)} \log h(g(x_{(i)}; \theta_p); \theta_a) + (1 - s_{(i)}) \log(1 - h(g(x_{(i)}; \theta_p); \theta_a)). \quad (13)$$

For a fixed encoder parameter θ_p , the adversary learns the optimal θ_a^* by maximizing (13). For a fixed θ_a , the encoder learns the optimal θ_p^* by minimizing $-L_n(h(g(X; \theta_p); \theta_a), S)$ subject to the distortion constraint $\mathbb{E}_{X, X_r} \|X - X_r\|^2 \leq D$.

As shown in Figure 2, the encoder is modeled by a two-layer neural network with parameters $\theta_p = \{\beta_0, \dots, \beta_m, \sigma_{p0}, \dots, \sigma_{pm}\}$, where β_k and σ_{pk} represent the mean and standard deviation for each dimension $k \in \{1, \dots, m\}$, respectively. The random noise Z is drawn from a m -dimensional independent zero-mean standard Gaussian distribution with covariance Σ_1 . Thus, we have $\hat{X}_k = X_k + \beta_k + \sigma_{pk} Z_k$. The adversary, whose goal is to infer S from privatized data X_r , is modeled by a three-layer neural network classifier with leaky ReLU activations.

To incorporate the distortion constraint into the learning process, we add a penalty term to the objective of the encoder. Thus, the training loss function of the encoder is given by

$$L(\theta_p, \theta_a) = L_n(\theta_p, \theta_a) + \rho \max \left\{ 0, \frac{1}{n} \sum_{i=1}^n d(g(x_{(i)}; \theta_p), x_{(i)}) - D \right\}, \quad (14)$$

where ρ is a penalty coefficient which increases with the number of iterations. The added penalty consists of a penalty parameter ρ multiplied by a measure of violation of the constraint. This measure of violation is non-zero when the constraint is violated. Otherwise, it is zero.

4.3 Illustration of Results

We use synthetic datasets to evaluate the performance of the learned representation by the CFUR framework. Each dataset contains $20K$ training samples and $2K$ test samples. Each data entry is sampled from an independent multi-dimensional Gaussian mixture model. We consider two categories of synthetic datasets with $P(S = 1)$ equal to 0.75 and 0.5, respectively. Both the encoder and the adversary in the CFUR framework are trained on Tensorflow Abadi et al. [2016] using Adam optimizer with a learning rate of 0.005 and a minibatch size of 1000. The distortion constraint is enforced by the penalty method as detailed in supplement B (see (38)).

Figure 3 illustrates the performance of the learned CFUR scheme against a strong theoretical MAP adversary for a 32-dimensional Gaussian mixture model with $P(S = 1) = 0.75$ and 0.5. We observe that the inference accuracy of the MAP adversary decreases as the distortion increases and asymptotically approaches (as expected) the prior on the sensitive variable. The decorrelation scheme obtained via the data-driven approach performs very well when pitted against the MAP adversary (maximum accuracy difference around 0.7% compared to the theoretical optimal). Furthermore, the estimated mutual information decreases as the distortion increases. In other words, for the data generated by Gaussian mixture model with binary sensitive variable, the data-driven version of the CFUR formulation can learn decorrelation schemes that perform as well as the decorrelation schemes computed under the theoretical version of the CFUR formulation, given that the generative decorrelator has access to the statistics of the dataset.

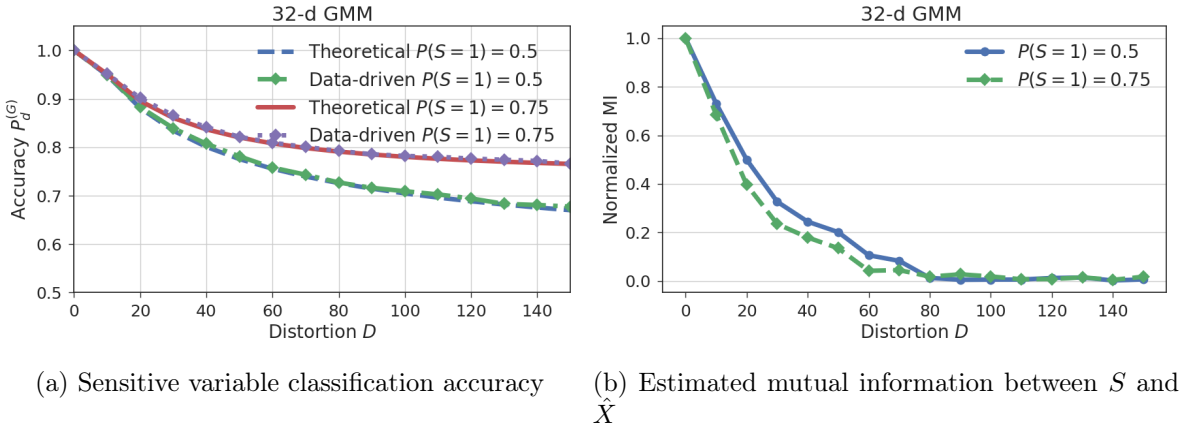


Figure 3: Performance of the CFUR framework for Gaussian mixture models

5 CFUR for Publicly Available Datasets

We apply our CFUR framework to real-world datasets including GENKI, HAR, UCI Adult and UTKFace:

- The GENKI dataset consists of 1,740 training and 200 test samples. Each data sample is a 16×16 greyscale face image with varying facial expressions. We consider gender² as the sensitive variable S and the image pixels as the non-sensitive variable X .
- The HAR dataset consists of 561 features of motion sensor data collected by a smartphone from 30 subjects performing six activities (walking, walking upstairs, walking downstairs,

²Even though gender is not binary, we treat it as a binary variable because the datasets we consider have examples only from males and females.

sitting, standing, laying). We choose subject identity as the sensitive variable S and features of motion sensor data as the non-sensitive variable X .

- The UCI Adult dataset³ is for salary prediction and consists of 10 categorical features and 4 continuous features. As shown in Table 5, we choose gender or the tuple (gender, relationship) as sensitive variable S and other features except salary as non-sensitive variable X .
- The UTKFace dataset⁴ consists of more than 20 thousand 200×200 colorful face images labeled by age, ethnicity and gender. Individuals in the dataset have ages from 0 to 116 years old and are divided into 5 ethnicities: White, Black, Asian, Indian, and others including Hispanic, Latino and Middle Eastern. We take gender as the sensitive variable S and the image pixels as the non-sensitive variable X .

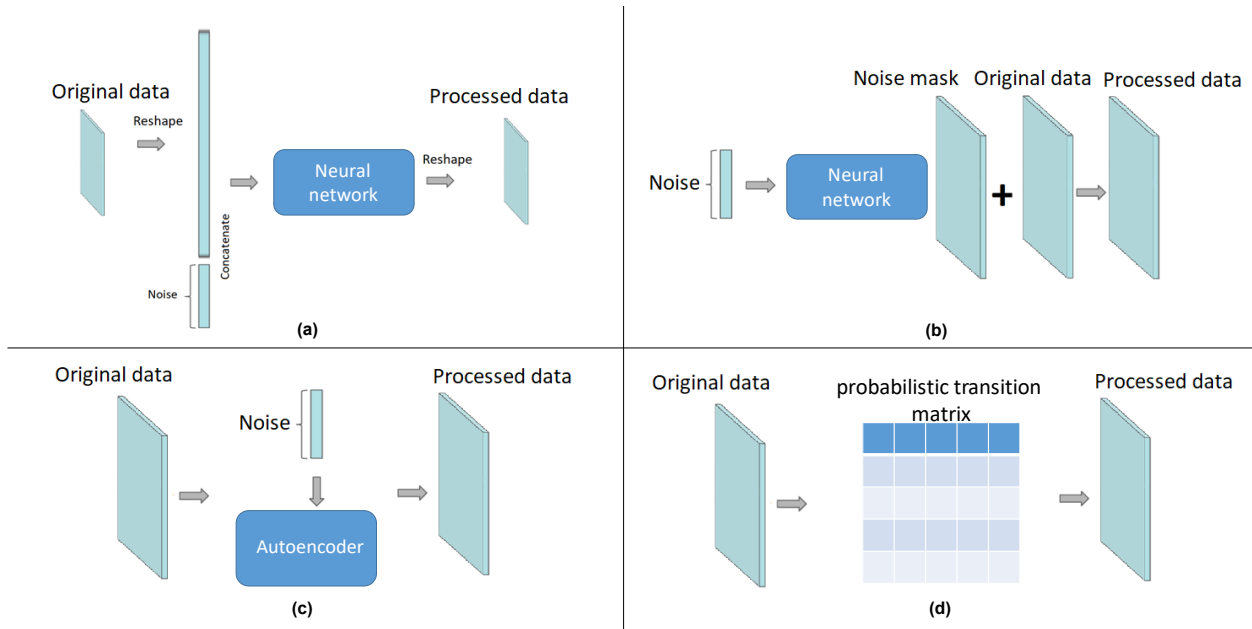


Figure 4: Different architectures of the decorrelator/encoder in the CFUR framework.

Three different architectures in Fig. 4 are used: the feedforward neural network decorrelator (FNND), the transposed convolution neural network decorrelator (TCNND) and the noisy autoencoder decorrelator (NAED). The FNND architecture (shown in Fig. 4 (a)) uses a feedforward multi-layer neural network to combine the low-dimensional random noise and the original data (i.e., X or (S, X)) together. The TCNND (shown in Fig. 4 (b)) generates a high-dimensional noise from a low-dimensional random noise by using a multi-layer transposed convolution neural network, and then, adds it to the original data to produce the representation X_r . The NAED (shown in Fig. 4 (c)) uses the encoder of an autoencoder to generate a lower-dimensional feature vector of the original data and adds independent random noise to each element of the feature vector. The decoder of the autoencoder reconverts the noisy feature vector to generate the processed data X_r . We apply both the FNND and TCNND architectures to the GENKI dataset. For the UCI Adult and HAR datasets, we use the FNND architecture, and the NAED architecture is applied to the UTKFace dataset.

³<https://archive.ics.uci.edu/ml/datasets/adult>

⁴<http://aicp.eecs.utk.edu/wiki/UTKFace>

We use the accuracy of predicting a sensitive feature as the measure of censoring. Demographic parity requires that the conditional probabilities of an arbitrary prediction $\hat{Y} = y$ for $y \in \mathcal{Y}$ given any $s \in \mathcal{S}$ equal. Therefore, for fairness, we take the following maximal difference as the measure of demographic parity, i.e.,

$$\Delta_{\text{DemP}}(y) = \max_{s, s' \in \mathcal{S}} |P(\hat{Y} = y|S = s) - P(\hat{Y} = y|S = s')| \quad (15)$$

and a smaller value of Δ_{DemP} implies a closer approaching of the demographic parity. We illustrate the results for each dataset mentioned above in the following subsections. Details of all experiments on these datasets are in Appendix F.

5.1 Illustration of Results for GENKI Dataset

Fig. 5a illustrates the gender classification accuracy of the adversary for different values of distortion. It can be seen that the adversary’s accuracy of classifying the sensitive variable (gender) decreases progressively as the distortion increases. Given the same distortion value, FNND achieves lower gender classification accuracy compared to TCNND. An intuitive explanation is that the FNND uses both the noise vector and the original image to generate the processed image. However, the TCNND generates the noise mask that is independent of the original image pixels and adds the noise mask to the original image in the final step.

Differential privacy has emerged as the gold standard for data privacy. In this experiment, we vary the variance of the Laplace and Gaussian noise to connect the noise adding mechanisms to local differential privacy [Duchi et al., 2013, Kairouz et al., 2016]. In particular, we compute the differential privacy guarantees provided by independent Laplace and Gaussian noise adding mechanisms for different distortion values. The details are provided in Appendix E. In Table 2, we observe that even if a huge amount of noise is added to each pixel of the image, the privacy risk (ϵ) is still high. Furthermore, adding a huge noise deteriorates the expression classification accuracy.

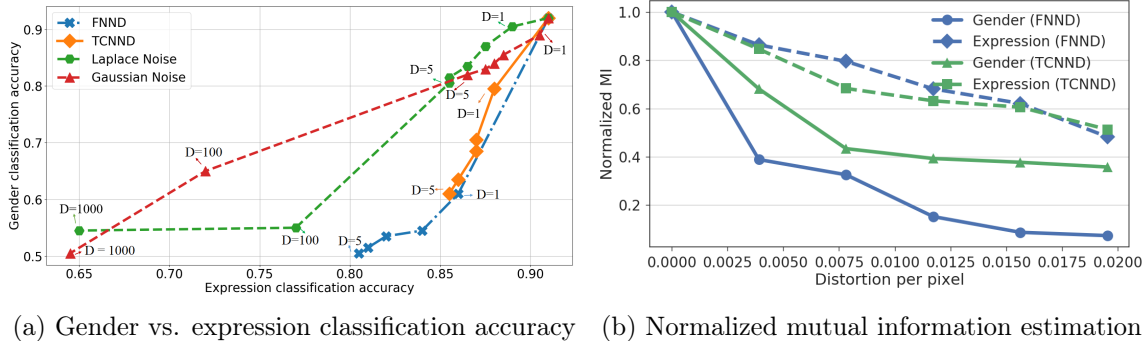


Figure 5: The tradeoff of classification accuracy and mutual information estimation for GENKI

To demonstrate the effectiveness of the learned CFUR schemes, we compare the gender classification accuracy of the learned CFUR schemes with adding uniform or Laplace noise. Fig. 5a shows that for the same distortion, the learned CFUR schemes achieve much lower gender classification accuracy than using uniform or Laplace noise. Furthermore, the estimated mutual information $\hat{I}(\hat{X}; S)$ normalized by $\hat{I}(X; S)$ also decreases as the distortion increases (Fig. 5b).

To evaluate the influence of the representation generated by the CFUR framework on other non-sensitive variable (Y) classification tasks, we train another CNN (see Figure 19) to perform facial expression classification on datasets processed by different decorrelation schemes. The trained model is then tested on the original test data. In Figure 5a, we observe that the expression classification

Distortion D	1	2	3	4	5	100	1000
Laplace Mechanism ϵ	5792.61	4096	3344.36	2896.31	2590.53	579.26	183.17
Gaussian Mechanism ($\delta = 10^{-6}$) ϵ	1918.24	1354.08	1107.57	959.18	857.76	191.82	60.66

Table 2: Differential privacy risk for different distortion values

Expression Classification	Original Data		D = 1		D = 3		D = 5	
	Male	Female	Male	Female	Male	Female	Male	Female
False Positive Rate	0.04	0.14	0.1	0.18	0.18	0.16	0.16	0.14
False Negative Rate	0.16	0.02	0.2	0.08	0.26	0.12	0.24	0.24

Table 3: Error rates for expression classification using representation learned by FNND

Expression Classification	Original Data		D = 1		D = 3		D = 5	
	Male	Female	Male	Female	Male	Female	Male	Female
False Positive Rate	0.04	0.14	0.04	0.16	0.06	0.12	0.08	0.16
False Negative Rate	0.16	0.02	0.2	0.08	0.2	0.14	0.18	0.16

Table 4: Error rates for expression classification using representation learned by TCNND

accuracy decreases gradually as the distortion increases. Even for a large distortion value (5 per image), the expression classification accuracy only decreases by 10%. Furthermore, the estimated normalized mutual information $\hat{I}(\hat{X}; Y)/\hat{I}(X; Y)$ decreases much slower than $\hat{I}(\hat{X}; S)/\hat{I}(X; S)$ as the distortion increases (Fig. 5b).

Tables 3 and 4 present different error rates for the facial expression classifiers trained using data representations created by different decorrelator architectures. For the GENKI dataset, smiling expression is considered as positive label for expression classification task. We observe that as distortion increases, the error rates difference for different sensitive groups decrease. This implies the classifier’s decision is less biased to the sensitive variables when trained using the processed data. When $D = 5$, the differences are already very small. Furthermore, we notice that the FNND architecture performs better in enforcing fairness but suffers from higher error rate. The images processed by FNND is shown in Fig. 6. The decorrelator changes mostly eyes, nose, mouth, beard, and hair.

5.2 Illustration of Results for HAR Dataset

Fig. 7a illustrates the activity and identity classification accuracy for different values of distortion. The adversary’s sensitive variable (identity) classification accuracy decreases progressively as the distortion increases. When the distortion is small ($D = 2$), the adversary’s classification accuracy is already around 27%. If we increase the distortion to 8, the classification accuracy further decreases to 3.8%. Fig. 7a depicts that even for a large distortion value ($D = 8$), the activity classification accuracy only decreases by 18% at most. Furthermore, Fig. 7b shows that the estimated normalized mutual information also decreases as the distortion increases.

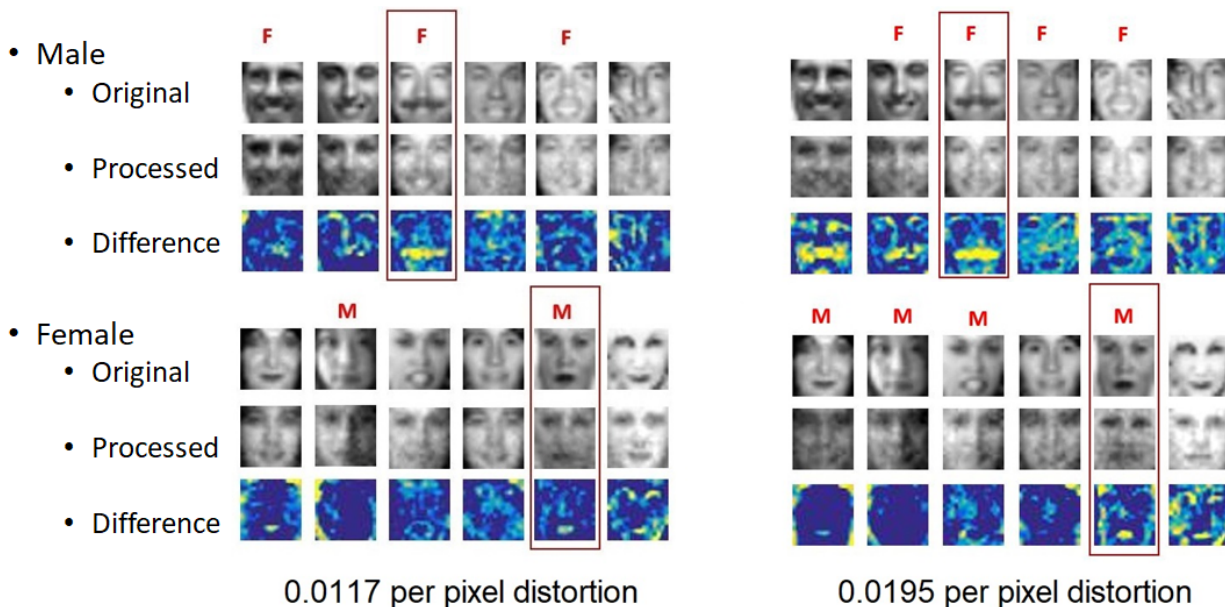


Figure 6: Perturbed images with different per pixel distortion using FNND

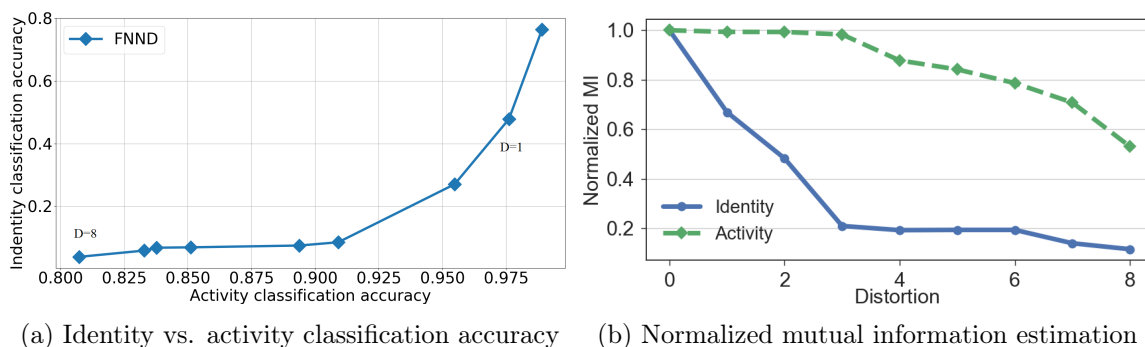


Figure 7: The tradeoff of classification accuracy and mutual information estimation for HAR

5.3 Illustration of Results for UCI Adult Dataset

For the UCI Adult dataset with both categorical and continuous features as shown in Table 5, we consider two cases: (i) in Case I, we take ‘gender’ as the sensitive variable S and S is either male or female in this dataset, and (ii) in Case II, we take both ‘gender’ and ‘relationship’ as the sensitive variable S . In this dataset, ‘relationship’ has 6 distinct values, and therefore, S has 12 possibilities. In both cases, we take ‘salary’ as the target variable Y , which is either $> 50K$ or $\leq 50K$. Note that for any binary target variable, the two values of the fair measure $\Delta_{\text{DemP}}(y)$ in (15) are the same, and therefore, we use Δ_{DemP} to denote the measure of demographic parity for experiments on this dataset.

Case I: Binary Sensitive Feature.

Fig. 8 illustrates the performances of the generated representation X_r for censoring and fairness concerns. Specifically, for censoring, the performance is evaluated via the tradeoff between the classification accuracy of salary and gender; and for fairness, it is evaluated via the tradeoff between the classification accuracy of salary and the demographic parity measure Δ_{DemP} . We consider two possible inputs of the encoder $g(\cdot)$ in (6), i.e., only the non-sensitive features X or both X and S .

From Fig. 8a, we observe that: (i) while the classification accuracy of gender (the sensitive

Case I	Feature	Description	Case II
Y	salary	2-salary intervals: $> 50K$ and $\leq 50K$	Y
S	gender	2 classes: male and female	S
X	relationship	6 classes of family relationships (e.g., wife and husband)	X
	age	9-age intervals: 18 – 25, 25 – 30, 30 – 35, ..., 60 – 65	
	workclass	8 types of employer	
	education	16 levels of the highest achieved education	
	marital-status	7 classes of marital status	
	occupation	14 types of occupation	
	race	5 classes	
	native-country	41 countries of origin	
	capital-gain	Recorded capital gain; (continuous)	
	capital-loss	Recorded capital loss; (continuous)	
	hours-per-week	Worked hours per week; (continuous)	
education-num	Numerical version of education; (continuous)		

Table 5: Features of the UCI Adult dataset

variable) is about 66% and only decreases about 20% from the baseline performance⁵, the classification accuracy of salary (the target variable) is above 82% and only decreases 2.5% from its baseline performance. Note that 66% is probability of male in the original testing data and indicates a random guess of gender. Therefore, the generated representation X_r hides the information of gender pretty well while maintaining the information of salary; (ii) only in the high utility region, where the accuracy of salary is no less than 72.5%, to take both S and X in the encoder $g(\cdot)$ has a small advantage over only using X . Specifically, given the same classification accuracy of gender, the classification accuracy of salary is at most 0.3% higher.

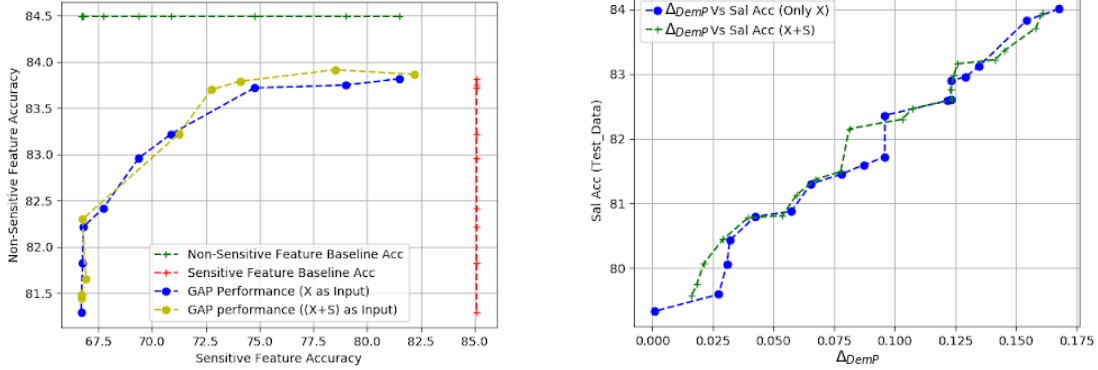
From Fig. 8b, we make the following two observations: (i) the classification accuracy of salary and the Δ_{DemP} have an approximately affine relationship, and when Δ_{DemP} is almost 0, the accuracy of salary is above 79%. Therefore, our framework is effective in approaching perfect demographic parity; (ii) the representation X_r generated from either X or (S, X) leads to a similar fairness performance. Comparing our results in Fig. 8b and the results in [Edwards and Storkey, 2016, Madras et al., 2018], for $\Delta_{\text{DemP}} = 0.06$, Edwards’ and Madras’s approaches have 2% and 2.5% higher classification accuracy of salary than ours, respectively. However, both their approaches are not shown to achieve the extreme point, $\Delta_{\text{DemP}} = 0$, but our approach does with the classification accuracy above 79%.

We can also evaluate the fairness performance of the generated representation by using equalized odds defined in Definition 1. Equalized odds requires that for both possible outcomes $Y = '> 50K'$ and $Y = '\leq 50K'$, the conditional probabilities of the correct prediction given the two possible gender (i.e., male or female) equal, i.e.,

$$\begin{aligned}
 P(\hat{Y} = Y | \text{female}, Y = '> 50K') &= P(\hat{Y} = Y | \text{male}, Y = '> 50K') \\
 P(\hat{Y} = Y | \text{female}, Y = '\leq 50K') &= P(\hat{Y} = Y | \text{male}, Y = '\leq 50K').
 \end{aligned}$$

Therefore, we use the differences of the above two pairs of conditional probabilities to characterize

⁵Note that the baseline performances are the accuracy or demographic parity measure obtained from the original testing data



(a) Salary vs. gender classification accuracy. (b) Salary classification accuracy vs. Δ_{DemP}

Figure 8: Performances for Case I of UCI Adult. Note that in Fig. 8a we use the classification accuracy for the original testing dataset (only using the non-sensitive feature X) as the baseline performance. The green and red lines denote the baseline performances for the target variable (salary) and the sensitive variable (gender), respectively; in Fig. 8b, the value of Δ_{DemP} for the original testing data is 0.2.

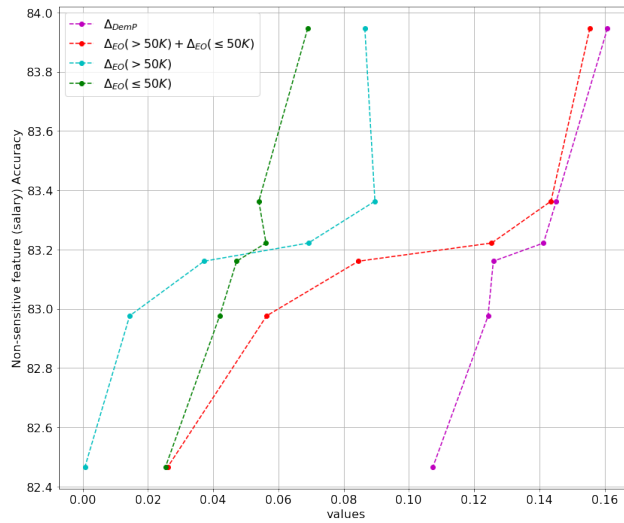


Figure 9: Evaluation of equalized odds fairness metric under Case I for the UCI Adult dataset. Note that $\Delta_{\text{EO}}(> 50K)$ and $\Delta_{\text{EO}}(\leq 50K)$ (defined in (16) and (17)) are the two measures of equalized odds for the two possible outcomes $Y = '> 50K'$ and $Y = '\leq 50K'$, respectively. The red curve is for the sum of $\Delta_{\text{EO}}(> 50K)$ and $\Delta_{\text{EO}}(\leq 50K)$, which is exactly the Δ_{EO} in Figure 2(b) of [Madras et al., 2018].

the achieved fairness in terms of equalized odds and define the two differences as

$$\Delta_{\text{EO}}(> 50K) \triangleq \left| P(\hat{Y} = Y | \text{female}, Y = '> 50K') - P(\hat{Y} = Y | \text{male}, Y = '> 50K') \right| \quad (16)$$

$$\Delta_{\text{EO}}(\leq 50K) \triangleq \left| P(\hat{Y} = Y | \text{female}, Y = '\leq 50K') - P(\hat{Y} = Y | \text{male}, Y = '\leq 50K') \right| \quad (17)$$

From the results in Fig. 9, we observe that while the classification accuracy of salary is above 82.4%, the values of $\Delta_{\text{EO}}(> 50K)$ and $\Delta_{\text{EO}}(\leq 50K)$ decrease to 0.0007 and 0.0254, respectively.

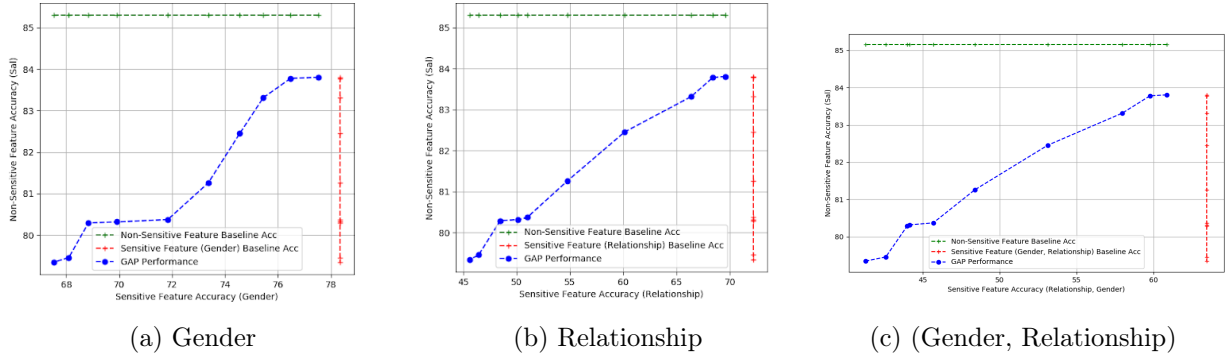


Figure 10: Tradeoff between classification accuracy of non-sensitive feature (salary) and sensitive features (gender and/or relationship) under Case II for the UCI Adult dataset. Note that we use the classification accuracy obtained from the original testing dataset as the baseline performance, which is denoted by the green and red lines for the target variable (salary) and the sensitive variable (gender or/and relationship), respectively.

Compare the sum of $\Delta_{\text{EO}}(> 50K)$ and $\Delta_{\text{EO}}(\leq 50K)$ with the value⁶ of Δ_{EO} in Figure 2(b) of [Madras et al., 2018], our representation generated under the rule of demographic parity is competitive with the method LAFTR-DP, which uses demographic parity as the fairness metric to train classification models. Specifically, when $\Delta_{\text{EO}}(> 50K) + \Delta_{\text{EO}}(\leq 50K) = 0.04$, our classification accuracy of salary is 1.3% smaller than the accuracy achieved by LAFTR-DP, but our minimal achieved value of $\Delta_{\text{EO}}(> 50K) + \Delta_{\text{EO}}(\leq 50K)$ is only 72% of that achieved by LAFTR-DP and the same as the value achieved by LAFTR-EO, which uses equalized odds as the fairness metric to train models. In addition, we observe that the decrease of $\Delta_{\text{EO}}(> 50K) + \Delta_{\text{EO}}(\leq 50K)$ is even larger than Δ_{DemP} . That is, even though the representation is generated under the rule of demographic parity, it provides a “guaranteed” fairness in terms of equalized odds. This, in turn, justifies the rationality of generating representations under the rule of demographic parity and also implies that to generate representations decorrelated with the sensitive feature while preserving the fidelity of the representations is a good method of providing fairness in terms of various metrics.

⁶Note that Δ_{EO} is the measure of equalized odds defined in [Madras et al., 2018] and $\Delta_{\text{EO}}(> 50K) + \Delta_{\text{EO}}(\leq 50K) = \Delta_{\text{EO}}$

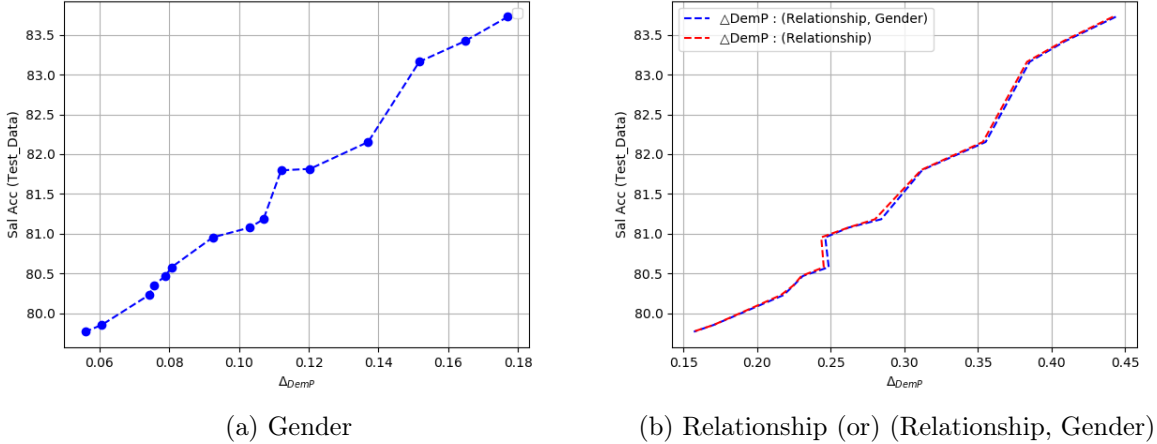


Figure 11: Tradeoffs between salary classification accuracy and the Δ_{DemP} of gender and/or relationship in Case II of UCI Adult. Note that in Fig. 11b, the red and blue lines are the demographic parity measure Δ_{DemP} for relationship and (gender, relationship), respectively. For the original testing data, the value of Δ_{DemP} for gender, relationship and (gender, relationship) is 0.2, 0.438 and 0.443, respectively.

Case II: Non-binary Sensitive Feature.

Figs. 10 and 11 illustrate the censoring and fairness performance of the generated representation X_r in hiding ‘gender’ and ‘relationship’ while preserves information of ‘salary’, respectively.

Fig. 10 shows the tradeoffs of the classification accuracy of salary versus gender, relationship, or their combination. From Fig. 10, we observe that while the classification accuracy of salary is above 79%, the classification accuracy of gender and/or relationship are about 66% (as shown in Fig. 10a), 45% (as shown in Fig. 10b) and 41% (as shown in Fig. 10c), respectively. Note that the probabilities of male, husband, and the combination (male, husband) is 66%, 40% and 40%, respectively, in the original testing data. Therefore, while the classification accuracy of salary is preserved as 79%, the inferences of gender, relationship, and combination (gender, relationship) are randomly guessing with known prior. Thus, the X_r is pretty well in hiding multiple sensitive information both separately and jointly. On the other hand, to have the flexibility of hiding the other sensitive information – relationship, the cost is a reduce in utility. Specifically, to compare the results in Figs. 8a and 10a, we can see that the drop of the classification accuracy of salary is at most 3% for any given accuracy of gender⁷.

Fig. 11 shows the tradeoffs between the classification accuracy of salary versus the demographic parity measure Δ_{DemP} (defined in (15)) *w.r.t.* gender, relationship or their combination⁸, respectively. We observe that while the classification accuracy of salary is above 94% of the baseline performance the value of Δ_{DemP} is dropped to 25% for gender and to about 34% for both relationship and the combination. Therefore, the X_r works well in decorrelating the information of salary and the information of gender and relationship jointly and separately. From 11b, we observe that the value of Δ_{DemP} for the combination is almost the same as that for relationship. In addition, comparing the results in Figs. 8b and 11b, we can see that for any given classification accuracy of salary, the Δ_{DemP} for gender in Case II can be about 25% higher of than that in Case I, which is

⁷Note that in Figs., 8a and 10a, the baseline performances are different and it is because in Case II, the feature variable X does not contain ‘relationship’.

⁸Note that there are no samples for (Female, Husband) and only 2 samples for (Male, Wife). Therefore, in the calculation of Δ_{DemP} , we ignore the two groups.

the cost of providing fairness for relationship.

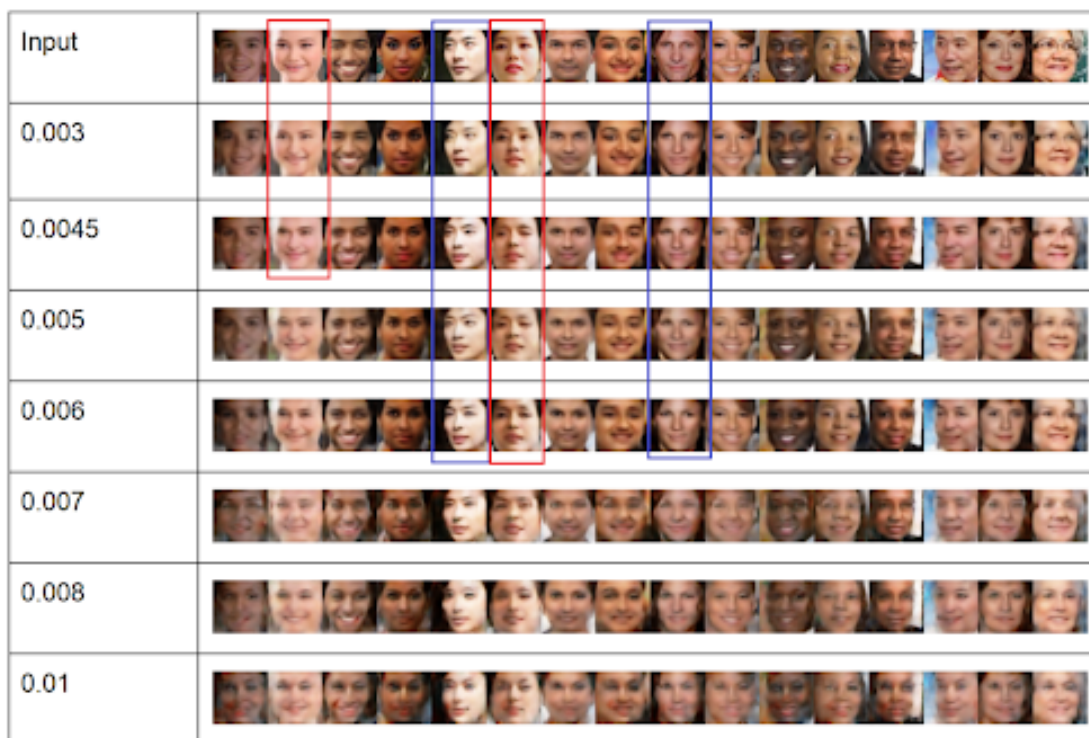


Figure 12: The encoded face images for different values of per-pixel distortions for the UTKFace dataset. Set of vertical faces highlighted in boxes make explicitly how the sensitive feature (gender) is changed with increasing distortion.

5.4 Illustration of Results for UTKFace Dataset

In the UTKFace dataset, the face images are the non-sensitive variable X . We take ‘gender’ as the sensitive variable S and either ‘ethnicity’ or ‘age’ as the target variable Y for ethnicity classification and age regression, respectively. For the two downstream applications, the corresponding supports of Y are $\mathcal{Y} = \{\text{White, Black, Asian, Indian}\}$ and $\mathcal{Y} = \{i \in \mathbb{Z} : 10 \leq i \leq 65\} = [10, 65]$, respectively. We use the maximum of the demographic parity measure (defined in (15)) over the support \mathcal{Y} , i.e., the value $\Delta_{\text{DemP}} = \max_{y \in \mathcal{Y}} \Delta_{\text{DemP}}(y)$, to indicate the achieved fairness.

Distortion	0	0.003	0.0045	0.005	0.006	0.007	0.008	0.01
$\Delta_{\text{DemP}}(\text{White})$	0.061	0.055	0.04	0.03	0.03	0.02	0.02	0.01
$\Delta_{\text{DemP}}(\text{Black})$	0.109	0.021	0.02	0.05	0.03	0.05	0.03	0.03
$\Delta_{\text{DemP}}(\text{Asian})$	0.14	0.082	0.07	0.07	0.06	0.07	0.06	0.03
$\Delta_{\text{DemP}}(\text{Indian})$	0.031	0.006	0.01	0	0.01	0	0.01	0.01

Table 6: Demographic parity fairness (indicated by $\Delta_{\text{DemP}}(\cdot)$) of ethnicity classification on the UTKFace dataset.

Figure 12 illustrates the output representations X_r for 16 typical⁹ faces in the UTKFace dataset

⁹The 16 typical faces covers the 8 possible combination of 2 gender (male and female) and 4 ethnicity (White, Black, Asian and Indian) and includes young, adult and old faces.

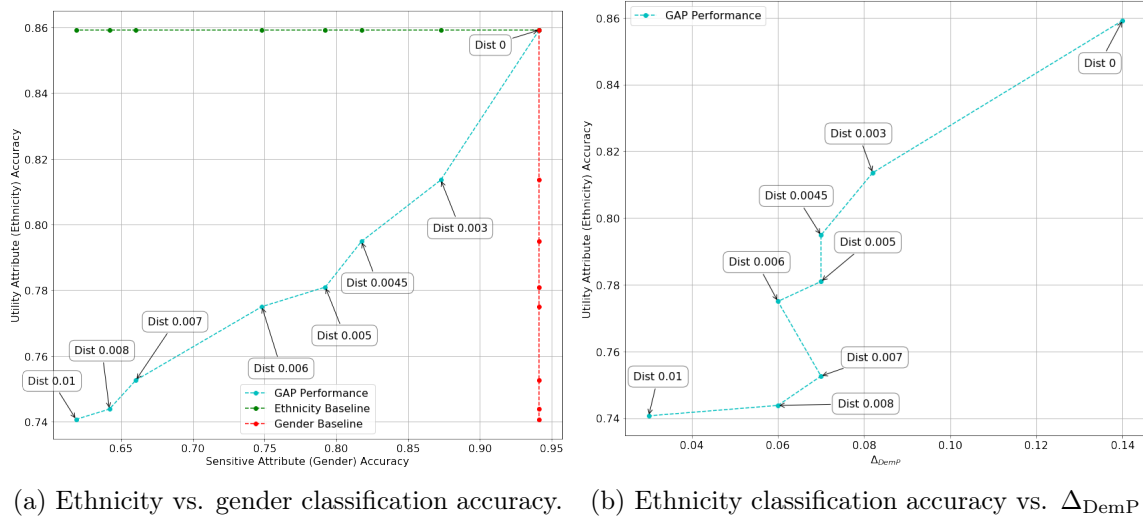


Figure 13: Ethnicity classification accuracy vs. gender classification and Δ_{DemP} for the UTKFace dataset. Note that in Fig. 13b, the x-axis is the maximal value of demographic parity measure in (15) over the four ethnicities and ‘dist’ indicate the per pixel distortion on images.

for increasing per-pixel distortion. From Fig. 12, we can observe (i) for a small per-pixel distortion (e.g., 0.003), the distinguished features of gender like lip color are smoothed out; and (ii) as a higher per-pixel distortion is allowed (e.g., 0.006), our framework generates a face with an opposite gender; (iii) however, when the average per-pixel distortion is too large (e.g., 0.01), the representation generated by the CFUR framework tends to be too blurred to show the face contour and clear five sense organs.

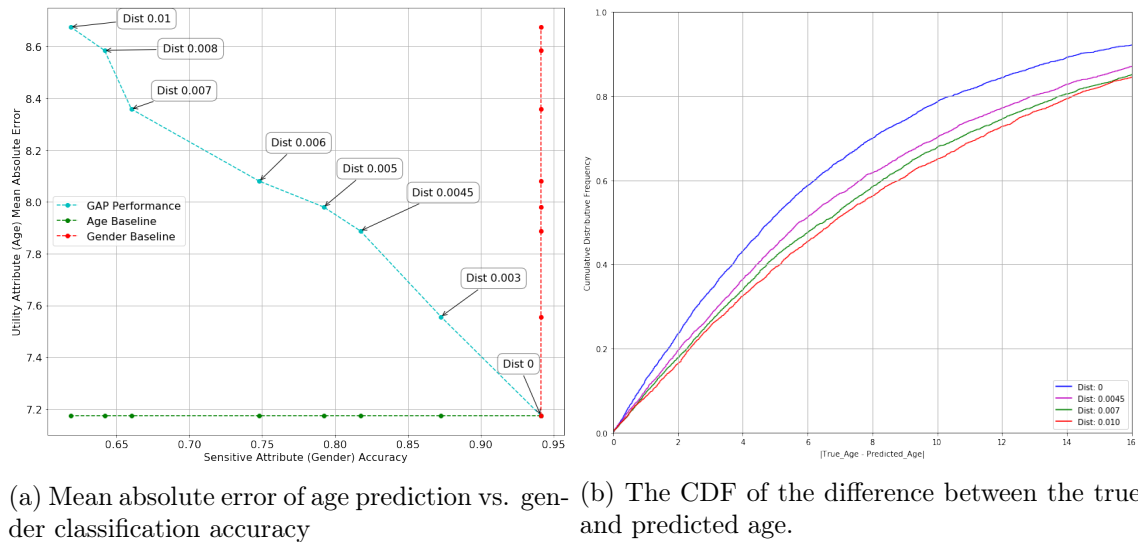
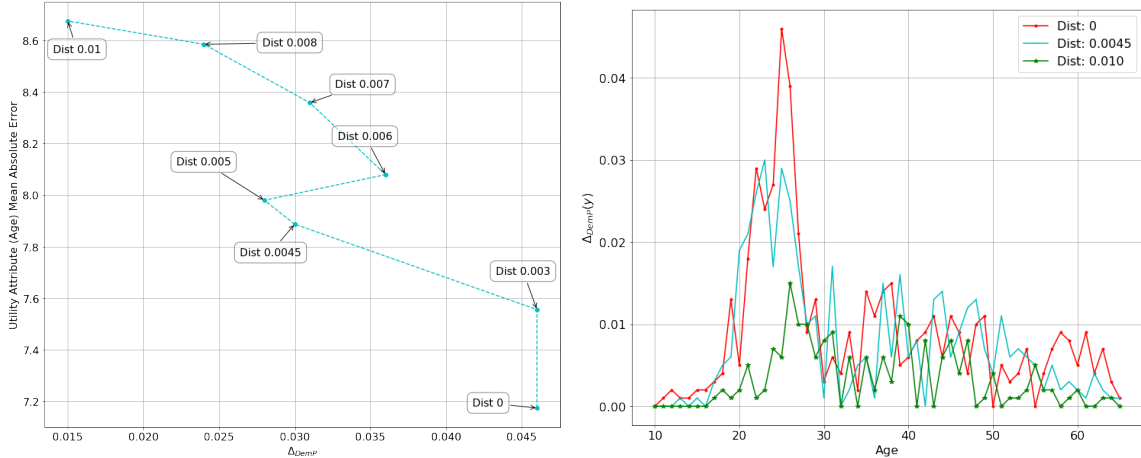


Figure 14: Utility of age regression on the UTKFace dataset. Note that ‘dist’ indicates the per pixel distortion on images.

Figs. 13a and 14 show the tradeoffs, achieved by the generated representation X_r , of the classification accuracy of gender and the utility for the ethnicity classification and age regression, respectively. In Fig. 13a, while the classification accuracy of gender is about 62% and decreases about 35% from the baseline performance, the classification accuracy of ethnicity is above 74% and only

decreases 14% from its baseline performance. Note that in the original testing data, the highest marginal probability for gender and ethnicity are 54.6% (the probability of male) and 43.2% (the probability of White), respectively. Therefore, the 62% classification accuracy of gender is only better than a random guess by 7.4% while the 74% classification accuracy of ethnicity is better than a random guess by 30.8%. Therefore, the X_r hides the information about gender well while maintaining the information about salary. For age regression, we use the mean absolute error (MAE), i.e., the average absolute difference between the predicted age and the true age, as the utility measure. In Fig. 14a, we observe that while the classification accuracy for gender is about 62%, which is a 35% decrease from the baseline performance 94%, the increase in the MAE is 1.5 which is about a 20% increase from the baseline performance 7.2. Fig. 14b shows the cumulative distribution function (CDF) of the difference between the true and predicted age for various distortions, from which we can see that the drop of the cumulative probability is at most 1%. Thus, it is shown that the CFUR framework also does a good job in maintaining the information about age, and therefore, constraining the distortion of generated representations is an efficient way for guaranteeing the utility of various applications.



(a) Mean absolute error of age prediction vs. Δ_{DemP} (b) The demographic parity measure for various distortions.

Figure 15: Achieved demographic parity for the age regression task on the UTKFace dataset. Note that in Fig. 15a, the x-axis is the maximal value of demographic parity measure in (15) over the chosen age range (10-65) and ‘dist’ indicate the per pixel distortion on images.

Figs. 13b and 15 show the tradeoff between the utility measure and demographic parity measure Δ_{DemP} of the generated representation X_r in ethnicity classification and age regression, respectively. In Fig. 13b, we observe that while achieving about 86% of the baseline classification accuracy, the Δ_{DemP} is reduced to 0.03 which is only 20% of the $\Delta_{DemP} = 0.14$ in the original testing data. Therefore, the X_r is good at approaching demographic parity fairness while maintaining the utility for ethnicity classification. Table 6 shows the decrease of the demographic parity measure for each the four ethnicity as the distortion increases. In Fig. 15a, while preserving 86% of the utility baseline performance, the Δ_{DemP} , i.e., the maximal value of demographic parity measure over the 56 age values, decreases to 0.015 which is less than 33% of the $\Delta_{DemP} = 0.046$ on the original testing data. Fig. 15b shows the demographic measure $\Delta_{DemP}(y)$, $y \in [10, 65]$, for various distortions, from which we observe that when the pixel distortion is 0.01, even though the $\Delta_{DemP} = 0.015$, for 17 different age values, $\Delta_{DemP}(y) = 0$. That is, the predictions of these 17 different ages are completely independent of gender (the sensitive information) and demographic parity is achieved

for those predictions.

6 Conclusion

We have introduced an adversarial learning framework with verifiable guarantees for learning ML models that can create censored and fair universal representations for datasets with known sensitive features. The novelty of our approach is in producing representations that are fair with respect to the sensitive features for any downstream learning task not known *a priori*. The CFUR framework allows the data holder to learn the fair encoding scheme (a randomized mapping that decorrelates the sensitive and non-sensitive features) directly from the dataset without requiring access to dataset statistics. Under the CFUR framework, finding the optimal encoder, subject to a fidelity constraint on the representation, is formulated as a constrained two-player game, namely a game between the generative encoder and an adversary. One of our key results is that for appropriately chosen loss functions, the CFUR framework can provide guarantees against strong information-theoretic adversaries, such as MAP (0-1 loss) and MI (log-loss) adversaries. It also allows enforcing fairness, quantified via demographic parity, via the tunable α -loss (which includes both log-loss and 0-1 loss) function. Furthermore, for *a priori* known classification task, we also proved that our CFUR framework can be modified to approximate fairness via demographic parity or equalized odds.

Yet another highlight of our work is the performance validation of the CFUR framework on both synthetic and publicly available real datasets including Gaussian mixture models, images, and datasets involving a mix of categorical and continuous features. Our results allow us to visually highlight two key results: (a) the tradeoff between representation fidelity and censoring guarantees (via adversarial learning of sensitive features); (b) the tradeoff between the adversarial accuracy in learning the sensitive features and the accuracy of multiple downstream tasks learned from the censored representation for a variety of datasets. Our results also reveal to some extent the effect on performance of the choice of encoder and adversary architectures (chosen as deep neural networks) for different datasets.

Going beyond this work, there are several fundamental questions that we seek to address. An immediate one is to develop techniques to rigorously benchmark data-driven results for large datasets against computable theoretical guarantees. More broadly, it will be interesting to investigate the robustness and convergence speed of the decorrelation schemes learned in a data-driven fashion.

Acknowledgments

We would like to acknowledge support for this project from the National Science Foundation via grants CCF-1422358, CCF-1350914, CIF-1815361 and CIF-1901243. We would also like to thank Prof. Ram Rajagopal and Xiao Chen at Stanford for their help with estimating mutual information for the GENKI and HAR datasets, and would like to thank Maunil Vyas, Mit Patel and Harshit Laddha at ASU for their help with the experiments on the UCI Adult and UTKFace datasets.

A Proof of Theorem 1

An encoder $g(X)$ that satisfies demographic parity ensures that X_r is independent of S , i.e., the mutual information $I(S; X_r) = 0$. Further, the downstream learning algorithm acts only on X_r to predict \hat{Y} ; combining these, we have that, $(S, X) - X_r - \hat{Y}$ form a Markov chain. From Definition 3, since X_r is independent of S , $I(S; X_r) = 0$. From the data processing inequality and non-negativity of mutual information, we have that,

$$0 \leq I(S; \hat{Y}) \leq I(S; X_r) = 0. \quad (18)$$

Therefore, S is independent of \hat{Y} , and thus, from Definition 1, \hat{Y} satisfies demographic parity w.r.t. S . Note that S can be a collection of sensitive features. From the fact $I(S; X_r) = 0$ as well as the chain rule and non-negativity of mutual information, we have $I(X_r; S_t) = 0$ for any subset of features $S_t \subset S$. Therefore, \hat{Y} satisfies demographic parity w.r.t. any subset of features in S .

B Theoretical Results of the CFUR Framework

Our CFUR framework places no restrictions on the adversary. Indeed, different loss functions and decision rules lead to different adversarial models. In what follows, we will discuss a variety of loss functions under hard and soft decision rules, and show how our CFUR framework provides censoring guarantees against various adversaries. We will also show that we can obtain a continuous interpolation between a hard-decision adversary under 0-1 loss function and a soft-decision adversary under log-loss function using the α -loss function.

Hard Decision Rules. When the adversary adopts a hard decision rule, $h(g(X))$ is an estimate of S . Under this setting, we can choose $\ell(h(g(X)), S)$ in a variety of ways. For instance, if S is continuous, the adversary can attempt to minimize the difference between the estimated and true sensitive variable values. This can be achieved by considering a squared loss function

$$\ell(h(g(X)), S) = (h(g(X)) - S)^2, \quad (19)$$

which is known as the ℓ_2 loss. In this case, one can verify that the adversary's optimal decision rule is $h^* = \mathbb{E}[S|g(X)]$, which is the conditional mean of S given $g(X)$. Furthermore, under the adversary's optimal decision rule, the minimax problem in (6) simplifies to

$$\min_{g(\cdot)} -\text{mmse}(S|g(X)) = -\max_{g(\cdot)} \text{mmse}(S|g(X)),$$

subject to the distortion constraint. Here $\text{mmse}(S|g(X))$ is the resulting minimum mean square error (MMSE) under $h^* = \mathbb{E}[S|g(X)]$. Thus, under the ℓ_2 loss, the CFUR framework provides censoring guarantees against an MMSE adversary. On the other hand, when S is discrete (e.g., age, gender, political affiliation, etc), the adversary can attempt to maximize its classification accuracy. This is achieved by considering a 0-1 loss function [Nguyen and Sanner, 2013] given by

$$\ell(h(g(X)), S) = \begin{cases} 0 & \text{if } h(g(X)) = S \\ 1 & \text{otherwise} \end{cases}. \quad (20)$$

In this case, one can verify that the adversary's optimal decision rule is the *maximum a posteriori probability* (MAP) decision rule: $h^* = \text{argmax}_{s \in \mathcal{S}} P(s|g(X))$, with ties broken uniformly at random. Moreover, under the MAP decision rule, the minimax problem in (6) reduces to

$$\min_{g(\cdot)} -(1 - \max_{s \in \mathcal{S}} P(s, g(X))) = \min_{g(\cdot)} \max_{s \in \mathcal{S}} P(s, g(X)) - 1, \quad (21)$$

subject to the distortion constraint. Thus, under a 0-1 loss function, the CFUR formulation provides censoring guarantees against a MAP adversary.

Soft Decision Rules. Instead of a *hard decision* rule, we can also consider a broader class of *soft decision* rules where $h(g(X))$ is a distribution over \mathcal{S} ; i.e., $h(g(X)) = P_h(s|g(X))$ for $s \in \mathcal{S}$. In this context, we can analyze the performance under a log-loss

$$\ell(h(g(X)), s) = \log \frac{1}{P_h(s|g(X))}. \quad (22)$$

In this case, the objective of the adversary simplifies to

$$\max_{h(\cdot)} -\mathbb{E}\left[\log \frac{1}{P_h(s|g(X))}\right] = -H(S|g(X)),$$

and that the maximization is attained at $P_h^*(s|g(X)) = P(s|g(X))$. Therefore, the optimal adversarial decision rule is determined by the true conditional distribution $P(s|g(X))$, which we assume is known to the data holder in the game-theoretic setting. Thus, under the log-loss function, the minimax optimization problem in (6) reduces to

$$\min_{g(\cdot)} -H(S|g(X)) = \min_{g(\cdot)} I(g(X); S) - H(S),$$

subject to the distortion constraint. Thus, under the log-loss in (22), the CFUR formulation is equivalent to using MI as the privacy metric [Calmon and Fawaz, 2012].

The 0-1 loss captures a strong guessing adversary; in contrast, log-loss or information-loss models a belief refining adversary.

B.1 Proof of Theorem 2

In (6), the output of the optimal encoder $g^*(X)$ is the universal representation of the original features X , i.e., $X_r = g^*(X) = \operatorname{argmin}_{g(\cdot)} \max_{h(\cdot)} -\mathbb{E}[\ell(h(g(X)); S)]$. Let h^* be the corresponding optimal adversarial strategy i.e., $h_{g^*}^* = \operatorname{argmin}_h \mathbb{E}[\ell(h(X_r), S)]$. For sufficient large distortion bound D , X_r can be arbitrarily distorted from X and $g(\cdot)$ can be any mapping from X to X_r . Therefore, we can get ride of the distortion constraint in (6) and have

$$-\mathbb{E}[\ell(h_{g^*}^*(X_r); S)] = -\max_{g(\cdot)} \min_{h(\cdot)} \mathbb{E}[\ell(h(g(X)); S)] \quad (23)$$

$$= -\max_{g(\cdot)} \mathbb{E}[\ell(h_g^*(g(X)); S)], \quad (24)$$

$$\leq -\mathbb{E}[\ell(h_g^*(g(X)); S)], \quad (25)$$

where $g(X)$ is any (randomized) mapping of X . That is, the generated representation X_r satisfies the inequality in (4). Thus, for sufficiently large distortion bound D , the generated representation X_r generated from the formulation in (6) is censored *w.r.t.* the sensitive variable S against a learning adversary $h(\cdot)$ captured by a loss function $\ell(h(X_r), S)$.

B.2 Proof of Proposition 1

Consider the α -loss function [Liao et al., 2018]

$$\ell(h(g(X)), s) = \frac{\alpha}{\alpha - 1} \left(1 - P_h(s|g(X))^{1-\frac{1}{\alpha}}\right), \quad (26)$$

for any $\alpha > 1$. Denote $H_\alpha^A(S|g(X))$ as the Arimoto conditional entropy of order α . Due to that α -loss is convex in $P_h(s|g(X))$, by using Karush–Kuhn–Tucker (KKT) conditions, we show that

$$\max_{h(\cdot)} -\mathbb{E}\left[\frac{\alpha}{\alpha-1}\left(1-P_h(s|g(X))^{1-\frac{1}{\alpha}}\right)\right] = \frac{\alpha}{1-\alpha}\left(1-\exp\left(\frac{1-\alpha}{\alpha}H_\alpha^A(S|g(X))\right)\right)$$

which is achieved by a ‘ α -tilted’ conditional distribution

$$P_h^*(s|g(X)) = \frac{P(s|g(X))^\alpha}{\sum_{s \in \mathcal{S}} P(s|g(X))^\alpha}.$$

Under this choice of a decision rule, the objective of the minimax optimization in (6) reduces to

$$\min_{g(\cdot)} -H_\alpha^A(S|g(X)). \quad (27)$$

B.3 Proof of Theorem 3

For any fixed classifier g , the optimal adversarial strategy in (6) is

$$h^*(g(X)) = \arg \max_{h(\cdot)} -\mathbb{E}[\ell(h(g(X)), S)]. \quad (28)$$

When α -loss is used, from Proposition. 1 we have that for $\alpha \geq 1$, the optimal adversarial strategy is given by

$$h^*(g(X), S) = \frac{P(s|g(X))^\alpha}{\sum_{s' \in \mathcal{S}} P(s'|g(X))^\alpha}, \quad (29)$$

for any $s \in \mathcal{S}$, and the corresponding expected α -loss is given by

$$\mathbb{E}[\ell(h(g(X)), S)] = \begin{cases} \frac{\alpha}{\alpha-1}\left(1-\exp\left(\frac{1-\alpha}{\alpha}H_\alpha^A(S|g(X))\right)\right), & \alpha > 1 \\ H(S|g(X)), & \alpha = 1. \end{cases} \quad (30)$$

Therefore, the optimization in (6) can be simplifies to

$$\min_{g(\cdot)} -H_\alpha^A(S|g(X)), \quad (31a)$$

$$\text{s.t. } \mathbb{E}[d(g(X), X)] \leq D \quad (31b)$$

where $H_\alpha^A(S|g(X))$ is the Arimoto conditional entropy of order α . Note that as α tends to 1, it simplifies to Shannon entropy [Verdú, 2015]. From the non-negativity of Arimoto mutual information, we know that

$$H_\alpha^A(S|g(X)) \leq H_\alpha^A(S) \quad (32)$$

with equality if and only if $g(X)$ is independent of S , which is exactly the requirement of demographic parity. Thus, as the distortion bound D in (31) increases, the CFUR formulation in (31) will approach ideal demographic parity by enforcing $H_\alpha^A(S|g(X)) = H_\alpha^A(S)$.

B.4 Proof of Theorem 2

For any fixed classifier \tilde{g} , the optimal adversarial strategy in (9) is

$$h^*(\tilde{g}(S, X), Y) = \arg \max_{h(\cdot)} -\mathbb{E}[\ell(h(\tilde{g}(S, X), Y), S)]. \quad (33)$$

When α -loss is used, from Proposition. 1 we have that for $\alpha \geq 1$, the optimal adversarial strategy is given by

$$h^*(\tilde{g}(S, X), Y) = \frac{P(s|\tilde{g}(S, X), Y)^\alpha}{\sum_{s' \in \mathcal{S}} P(s'|\tilde{g}(S, X), Y)^\alpha}, \quad (34)$$

for any $s \in \mathcal{S}$, and the corresponding expected α -loss is given by

$$\mathbb{E}[\ell(h(\tilde{g}(S, X), Y), S)] = \begin{cases} \frac{\alpha}{\alpha-1} (1 - \exp(-\frac{1-\alpha}{\alpha} H_\alpha^A(S|\tilde{g}(S, X), Y))), & \alpha > 1 \\ H(S|\tilde{g}(S, X), Y), & \alpha = 1. \end{cases} \quad (35)$$

Therefore, the optimization in (9) can be simplified to

$$\min_{\tilde{g}(\cdot)} -H_\alpha^A(S|\tilde{g}(S, X), Y), \quad (36a)$$

$$\text{s.t. } \mathbb{E}[\ell(\tilde{g}(S, X), Y)] \leq L \quad (36b)$$

where $H_\alpha^A(S|\tilde{g}(S, X), Y)$ is the Arimoto conditional entropy of order α . Note that as α tends to 1, it simplifies to Shannon entropy [Verdú, 2015].

From the non-negativity of Arimoto mutual information, we know that

$$H_\alpha^A(S|\tilde{g}(S, X), Y) \leq H_\alpha^A(S|Y) \quad (37)$$

with equality if and only if $\tilde{g}(S, X)$ is independent of S conditioning on Y , which is exactly the requirement of equalized odds. Thus, as the loss upper-bound L in (36) increases, the CFUR formulation in (36) will approach ideal equalized odds of $\tilde{g}(S, X)$ respect to Y and S by enforcing $H_\alpha^A(S|\tilde{g}(S, X), Y) = H_\alpha^A(S|Y)$.

C Alternate Minimax Algorithm

In this section, we present the alternate minimax algorithm to learn the CFUR model from a dataset. The alternating minimax censoring preserving algorithm is presented in Algorithm 1. To incorporate the distortion constraint into the learning algorithm, we use the *penalty method* [Lillo et al., 1993] and *augmented Lagrangian method* [Eckstein and Yao, 2012] to replace the constrained optimization problem by a series of unconstrained problems whose solutions asymptotically converge to the solution of the constrained problem. Under the penalty method, the unconstrained optimization problem is formed by adding a penalty to the objective function. The added penalty consists of a penalty parameter ρ_t multiplied by a measure of violation of the constraint. The measure of violation is non-zero when the constraint is violated and is zero if the constraint is not violated. Therefore, in Algorithm 1, the constrained optimization problem of the decorrelator can be approximated by a series of unconstrained optimization problems with the loss function

$$\ell(\theta_p^t, \theta_a^{t+1}) = -\frac{1}{M} \sum_{i=1}^M \ell(h(g(x_{(i)}; \theta_p^t); \theta_a^{t+1}), s_{(i)}) + \rho_t (\max\{0, \frac{1}{M} \sum_{i=1}^M d(g(x_{(i)}; \theta_p^t), x_{(i)}) - D\})^2, \quad (38)$$

Algorithm 1 Alternating minimax censoring preserving algorithm

Input: dataset \mathcal{D} , distortion parameter D , iteration number T

Output: Optimal generative decorrelator parameter θ_p

procedure ALERNATE MINIMAX(\mathcal{D}, D, T)

Initialize θ_p^1 and θ_a^1

for $t = 1, \dots, T$ **do**

Random minibatch of M datapoints $\{x_{(1)}, \dots, x_{(M)}\}$ drawn from full dataset

Generate $\{\hat{x}_{(1)}, \dots, \hat{x}_{(M)}\}$ via $\hat{x}_{(i)} = g(x_{(i)}; \theta_p^t)$

Update the adversary parameter θ_a^{t+1} by stochastic gradient ascend for j epochs

$$\theta_a^{t+1} = \theta_a^t + \alpha_t \nabla_{\theta_a^t} \frac{1}{M} \sum_{i=1}^M -\ell(h(\hat{x}_{(i)}; \theta_a^t), s_{(i)}), \quad \alpha_t > 0$$

Compute the descent direction $\nabla_{\theta_p^t} \ell(\theta_p^t, \theta_a^{t+1})$, where

$$\ell(\theta_p^t, \theta_a^{t+1}) = -\frac{1}{M} \sum_{i=1}^M \ell(h(g(x_{(i)}; \theta_p^t); \theta_a^{t+1}), s_{(i)})$$

subject to $\frac{1}{M} \sum_{i=1}^M [d(g(x_{(i)}; \theta_p^t), x_{(i)})] \leq D$

Perform line search along $\nabla_{\theta_p^t} \ell(\theta_p^t, \theta_a^{t+1})$ and update

$$\theta_p^{t+1} = \theta_p^t - \alpha_t \nabla_{\theta_p^t} \ell(\theta_p^t, \theta_a^{t+1})$$

Exit if solution converged

end for

return θ_p^{t+1}

end procedure

where ρ_t is a penalty coefficient which increases with the number of iterations t . For convex optimization problems, the solution to the series of unconstrained problems will eventually converge to the solution of the original constrained problem [Lillo et al., 1993].

The augmented Lagrangian method is another approach to enforce equality constraints by penalizing the objective function whenever the constraints are not satisfied. Different from the penalty method, the augmented Lagrangian method combines the use of a Lagrange multiplier and a quadratic penalty term. Note that this method is designed for equality constraints. Therefore, we introduce a slack variable δ to convert the inequality distortion constraint into an equality constraint. Using the augmented Lagrangian method, the constrained optimization problem of the decorrelator can be replaced by a series of unconstrained problems with the loss function given by

$$\begin{aligned} \ell(\theta_p^t, \theta_a^{t+1}, \delta) = & -\frac{1}{M} \sum_{i=1}^M \ell(h(g(x_{(i)}; \theta_p^t); \theta_a^{t+1}), s_{(i)}) + \frac{\rho_t}{2} \left(\frac{1}{M} \sum_{i=1}^M d(g(x_{(i)}; \theta_p^t), x_{(i)}) + \delta - D \right)^2 \\ & - \lambda_t \left(\frac{1}{M} \sum_{i=1}^M d(g(x_{(i)}; \theta_p^t), x_{(i)}) + \delta - D \right), \end{aligned} \quad (39)$$

where ρ_t is a penalty coefficient which increases with the number of iterations t and λ_t is updated according to the rule $\lambda_{t+1} = \lambda_t - \rho_t (\frac{1}{M} \sum_{i=1}^M d(g(x_{(i)}; \theta_p^t), x_{(i)}) + \delta - D)$. For convex optimization problems, the solution to the series of unconstrained problems formulated by the augmented Lagrangian method also converges to the solution of the original constrained problem [Eckstein and Yao, 2012].

C.1 Proof of Theorem 4

Since $\mathbb{E}_{X, \hat{X}}[d(\hat{X}, X)] = \mathbb{E}_{X, \hat{X}}\|X - \hat{X}\|^2 = \mathbb{E}\|Z + \beta\|^2 = \|\beta\|^2 + \text{tr}(\Sigma_p)$, the distortion constraint implies that $\|\beta\|^2 + \text{tr}(\Sigma_p) \leq D$. Let us consider $\hat{X} = X + Z + \beta$, where $\beta \in \mathbb{R}$ and Σ_p is a diagonal covariance whose diagonal entries is given by $\{\sigma_{p_1}^2, \dots, \sigma_{p_m}^2\}$. Given the MAP adversary's optimal inference accuracy in (12), the objective of the decorrelator is to

$$\begin{aligned} \min_{\beta, \Sigma_p} P_d^{(G)} \quad (40) \\ \text{s.t.} \quad \|\beta\|^2 + \text{tr}(\Sigma_p) \leq D. \end{aligned}$$

Define $\frac{1-q}{q} = \eta$. The gradient of $P_d^{(G)}$ w.r.t. α is given by

$$\frac{\partial P_d^{(G)}}{\partial \alpha} = \tilde{p} \left(-\frac{1}{\sqrt{2\pi}} e^{-\frac{(-\frac{\alpha}{2} + \frac{1}{\alpha} \ln \eta)^2}{2}} \right) \left(-\frac{1}{2} - \frac{1}{\alpha^2} \ln \eta \right) \quad (41)$$

$$\begin{aligned} &+ (1 - \tilde{p}) \left(-\frac{1}{\sqrt{2\pi}} e^{-\frac{(-\frac{\alpha}{2} - \frac{1}{\alpha} \ln \eta)^2}{2}} \right) \left(-\frac{1}{2} + \frac{1}{\alpha^2} \ln \eta \right) \\ &= \frac{1}{2\sqrt{2\pi}} \left(\tilde{p} e^{-\frac{(-\frac{\alpha}{2} + \frac{1}{\alpha} \ln \eta)^2}{2}} + (1 - \tilde{p}) e^{-\frac{(-\frac{\alpha}{2} - \frac{1}{\alpha} \ln \eta)^2}{2}} \right) \quad (42) \\ &+ \frac{\ln \eta}{\alpha^2 \sqrt{2\pi}} \left(\tilde{p} e^{-\frac{(-\frac{\alpha}{2} + \frac{1}{\alpha} \ln \eta)^2}{2}} - (1 - \tilde{p}) e^{-\frac{(-\frac{\alpha}{2} - \frac{1}{\alpha} \ln \eta)^2}{2}} \right). \end{aligned}$$

Note that

$$\frac{\tilde{p} e^{-\frac{(-\frac{\alpha}{2} + \frac{1}{\alpha} \ln \eta)^2}{2}}}{(1 - \tilde{p}) e^{-\frac{(-\frac{\alpha}{2} - \frac{1}{\alpha} \ln \eta)^2}{2}}} = \frac{\tilde{p}}{1 - \tilde{p}} e^{\frac{(-\frac{\alpha}{2} - \frac{1}{\alpha} \ln \eta)^2 - (-\frac{\alpha}{2} + \frac{1}{\alpha} \ln \eta)^2}{2}} = \frac{\tilde{p}}{1 - \tilde{p}} e^{\frac{2 \ln \eta}{2}} = \frac{\tilde{p}}{1 - \tilde{p}} e^{\ln \eta} = 1. \quad (43)$$

Therefore, the second term in (42) is 0. Furthermore, the first term in (42) is always positive. Thus, $P_d^{(G)}$ is monotonically increasing in α . As a result, the optimization problem in (40) is equivalent to

$$\begin{aligned} \min_{\beta, \Sigma_p} (2\mu)^T (\Sigma + \Sigma_p)^{-1} 2\mu \quad (44) \\ \text{s.t.} \quad \|\beta\|^2 + \text{tr}(\Sigma_p) \leq D. \end{aligned}$$

The objective function in (44) can be written as

$$2 \begin{bmatrix} \mu_1 & \mu_2 & \dots & \mu_m \end{bmatrix} \begin{bmatrix} \frac{1}{\sigma_1^2 + \sigma_{p_1}^2} & 0 & \dots & 0 \\ 0 & \frac{1}{\sigma_2^2 + \sigma_{p_2}^2} & \dots & 0 \\ \vdots & \vdots & \ddots & \vdots \\ 0 & 0 & \dots & \frac{1}{\sigma_m^2 + \sigma_{p_m}^2} \end{bmatrix} 2 \begin{bmatrix} \mu_1 \\ \mu_2 \\ \vdots \\ \mu_m \end{bmatrix} = \sum_{i=1}^m \frac{4\mu_i^2}{\sigma_i^2 + \sigma_{p_i}^2}.$$

Thus, the optimization problem in (44) is equivalent to

$$\begin{aligned} \min_{\beta, \sigma_{p_1}^2, \dots, \sigma_{p_m}^2} \quad & \sum_{i=1}^m \frac{\mu_i^2}{\sigma_i^2 + \sigma_{p_i}^2} \\ \text{s.t.} \quad & \|\beta\|^2 + \text{tr}(\Sigma_p) \leq D \\ & \sigma_{p_i}^2 \geq 0 \quad \forall i \in \{1, 2, \dots, m\}. \end{aligned} \quad (45)$$

Since a non-zero β does not affect the objective function but result in positive distortion, the optimal scheme satisfies $\beta = (0, \dots, 0)$. Furthermore, the Lagrangian of the above optimization problem is given by

$$L(\sigma_{p_1}^2, \dots, \sigma_{p_m}^2, \lambda) = \sum_{i=1}^m \frac{\mu_i^2}{\sigma_i^2 + \sigma_{p_i}^2} + \lambda_0 \left(\sum_{i=1}^m \sigma_{p_i}^2 - D \right) - \sum_{i=1}^m \lambda_i \sigma_{p_i}^2, \quad (46)$$

where $\lambda = \{\lambda_0, \dots, \lambda_m\}$ denotes the Lagrangian multipliers associated with the constraints. Taking the derivatives of $L(\sigma_{p_1}^2, \dots, \sigma_{p_m}^2, \lambda)$ with respect to $\sigma_{p_i}^2, \forall i \in \{1, \dots, m\}$, we have

$$\frac{\partial L(\sigma_{p_1}^2, \dots, \sigma_{p_m}^2, \lambda)}{\partial \sigma_{p_i}^2} = -\frac{\mu_i^2}{(\sigma_i^2 + \sigma_{p_i}^2)^2} + \lambda_0 - \lambda_i. \quad (47)$$

Notice that the objective function in (44) is decreasing in $\sigma_{p_i}^2, \forall i \in \{1, \dots, m\}$. Thus, the optimal solution $\sigma_{p_i}^{*2}$ satisfies $\sum_{i=1}^m \sigma_{p_i}^{*2} = D$. By the KKT conditions, we have

$$\left. \frac{\partial L(\sigma_{p_1}^2, \dots, \sigma_{p_m}^2, \lambda)}{\partial \sigma_{p_i}^2} \right|_{\sigma_{p_i}^2 = \sigma_{p_i}^{*2}, \lambda = \lambda^*} = -\frac{\mu_i^2}{(\sigma_i^2 + \sigma_{p_i}^{*2})^2} + \lambda_0^* - \lambda_i^* = 0. \quad (48)$$

Since $\lambda_i^*, i \in \{0, 1, \dots, m\}$ is dual feasible, we have $\lambda_i^* \geq 0, i \in \{0, 1, \dots, m\}$. Therefore

$$\lambda_0^* \geq \frac{\mu_i^2}{(\sigma_i^2 + \sigma_{p_i}^{*2})^2}.$$

If $\lambda_0^* > \frac{\mu_i^2}{\sigma_i^4}$, we have $\lambda_0^* > \frac{\mu_i^2}{(\sigma_i^2 + \sigma_{p_i}^{*2})^2}$. This implies $\lambda_i^* > 0$. Thus, by complementary slackness, $\sigma_{p_i}^{*2} = 0$. On the other hand, if $\lambda_0^* < \frac{\mu_i^2}{\sigma_i^4}$, we have $\sigma_{p_i}^{*2} > 0$. Furthermore, by the complementary slackness condition, $\lambda_i^* \sigma_{p_i}^{*2} = 0, \forall \sigma_{p_i}^{*2}$. This implies $\lambda_i^* = 0, \forall \sigma_{p_i}^{*2} > 0$. As a result, for all $\sigma_{p_i}^{*2} > 0$, we have

$$\frac{|\mu_i|}{\sqrt{\lambda_0^*}} = \sigma_i^2 + \sigma_{p_i}^{*2}. \quad (49)$$

Therefore, $\sigma_{p_i}^{*2} = \max\left\{\frac{|\mu_i|}{\sqrt{\lambda_0^*}} - \sigma_i^2, 0\right\} = \left(\frac{|\mu_i|}{\sqrt{\lambda_0^*}} - \sigma_i^2\right)^+$ with $\sum_{i=1}^m \sigma_{p_i}^{*2} = D$. Substitute this optimal solution into (12) with $\alpha = \sqrt{(2\mu)^T(\Sigma + \Sigma_p)^{-1}2\mu}$, we obtain the accuracy of the MAP adversary.

We observe that the when σ_i^2 is greater than some threshold $\frac{|\mu_i|}{\sqrt{\lambda_0^*}}$, no noise is added to the data on this dimension due to the high variance. When σ_i^2 is smaller than $\frac{|\mu_i|}{\sqrt{\lambda_0^*}}$, the amount of noise added to this dimension is proportional to $|\mu_i|$; this is intuitive since a large $|\mu_i|$ indicates the two conditionally Gaussian distributions are further away on this dimension, and thus, distinguishable. Thus, more noise needs to be added in order to reduce the MAP adversary's inference accuracy.

D Mutual Information Estimation

Our CFUR framework offers a scalable way to find a (local) equilibrium in the constrained min-max optimization, under certain attacks (e.g. attacks based on a neural network). Yet the privatized data, through our approach, should be immune to any general attacks and ultimately achieving the goal of decreasing the correlation between the privatized data and the sensitive labels. Therefore we use the estimated mutual information to certify that the sensitive data indeed is protected via our framework.

We use the nearest k -th neighbor method [Kraskov et al., 2004] to estimate the entropy \hat{H} given by

$$\hat{H}(\hat{X}) = \psi(N) - \psi(k) + \log(c_d) + \frac{d}{N} \sum_{i=1}^N \log r_i \quad (50)$$

where r_i is the distance of the i -th sample \hat{x}_i to its k -th nearest neighbor, ψ is the digamma function, $c_d = \frac{\pi^{d/2}}{\Gamma(1+d/2)}$ in Euclidean norm, and N is the number of samples. Notice that \hat{X} is learned representation and S is the sensitive variable. Then, we calculate the mutual information using $\hat{I}(\hat{X}; S) = \hat{H}(\hat{X}) - \hat{H}(\hat{X}|S)$

For a binary sensitive variable, we can simplify the empirical MI to

$$\hat{I}(\hat{X}; S) = \hat{H}(\hat{X}) - (P(S=1)\hat{H}(\hat{X}|S=1) + P(S=0)\hat{H}(\hat{X}|S=0)), \quad (51)$$

where $P(S=1)$ and $P(S=0)$ can be approximated by the empirical probability.

One noteworthy difficulty is that \hat{X} usually lives in high dimensions (e.g. each image has 256 dimensions in GENKI dataset) which is almost impossible to calculate the empirical entropy based on raw data due to the sample complexity. Thus, we train a neural network that classifies the sensitive variable from the learned data representation to reduce the dimension of the data. We choose the layer before the softmax outputs (denoted by \hat{X}_f) to be the feature embedding that has a much lower dimension than original \hat{X} and also captures the information about the sensitive variable. We use \hat{X}_f as a surrogate of \hat{X} for estimating the entropy. The resulting approximate MI is

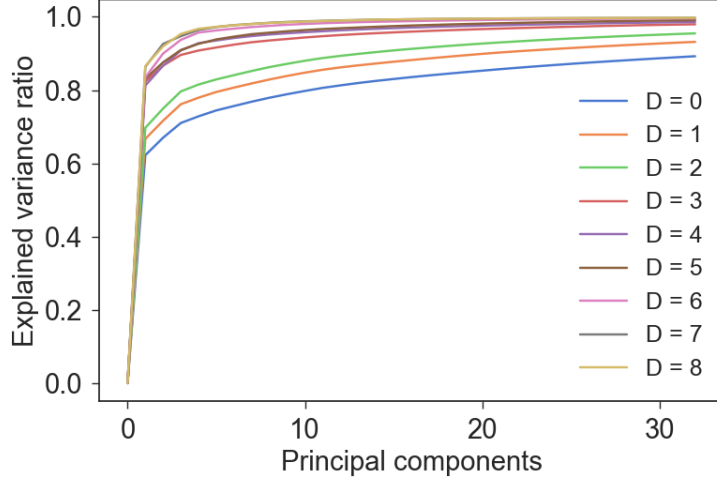
$$\begin{aligned} \hat{I}(\hat{X}_f; S) &= \hat{H}(\hat{X}_f) - \hat{H}(\hat{X}_f|S) \\ &= \hat{H}(\hat{X}_f) - (P(S=1)\hat{H}(\hat{X}_f|S=1) + P(S=0)\hat{H}(\hat{X}_f|S=0)). \end{aligned}$$

Following the same manner, the MI between the learned representation \hat{X} and the label Y is approximated by $\hat{I}(\hat{X}_f; Y)$, where \hat{X}_f is the feature embedding that represents a privatized image \hat{X} .

For the GENKI dataset, we construct a CNN initialized by two conv blocks, then followed by two fully connected (FC) layers, and lastly ended with two neurons having the softmax activations. In each conv block, we have a convolution layer consisting of filters with the size equals 3×3 and the stride equals 1, a 2×2 max-pooling layer with the stride equals 2, and a ReLU activation function. Those two conv blocks have 32 and 64 filters respectively. We flatten out the output of second conv block yielding a 256 dimension vector. The extracted features from the second conv layers is passed through the first FC layer with batch normalization and ReLU activation to get a 8-dimensional vector, followed with the second FC layer to output a 2 dimensional vector that applied with the softmax function. The aforementioned 8-dimensional vector is the feature embedding vector \hat{X}_f in our empirical MI estimation.

Estimating mutual information for HAR dataset has a slightly different challenge, as the size of the alphabet for the sensitive label (i.e. identity) is 30. Thus, it requires at least 30 neurons

prior to the output layer of the corresponding classification task. In fact we pose 128 neurons before the final softmax output layer in order to get a reasonably good classification accuracy. Using the 128-dimensional vector as our feature embedding to calculate mutual information is almost impossible due to the curse of dimensionality. Therefore, we apply Principal Component Analysis (PCA), shown in Figure 16, and pick the first 12 components to circumvent this issue. The resulting 12-dimensional vector is considered to be an approximate feature embedding that encapsulates the major information of the processed data.



(a) Top 32 principal components out of the 561 features with different distortion D

Figure 16: PCA for processed data in HAR

E Compute differential censoring risk for the Laplace and Gaussian noise adding mechanisms

In the local differential privacy setting, we consider the value of each pixel as the output of the query function. Since the pixel values of the GENKI dataset are normalized between 0 and 1, we can use the dimension of the image to bound the sensitivities for both Laplace mechanism and Gaussian mechanism. For the Laplace mechanism, let X and X' be two different image vectors. Since the value of X and X' in each dimension is between 0 and 1, $|X_i - X'_i| \leq 1$ for the i^{th} dimension. Thus, the L_1 sensitivity can be bounded by the dimension of the image d . Notice that the variance of the Laplace noise parameterized by λ is $2\lambda^2$. Since we are adding independent Laplace noise to each pixel, given the per image distortion D , we have

$$\frac{D}{d} = 2 \frac{d^2}{\epsilon^2} \implies \epsilon = d \sqrt{\frac{2d}{D}}.$$

Similarly, for the Gaussian mechanism, we can bound the L_2 sensitivity by \sqrt{d} . For a fixed δ , the privacy risk ϵ for adding Gaussian noise with variance σ^2 is given by

$$\epsilon = 2 \frac{\sqrt{d}}{\sigma} \sqrt{\ln\left(\frac{1.25}{\delta}\right)}.$$

Since we are adding Gaussian noise independently to each pixel, the variance of the per pixel noise is given by $\sigma = \frac{D}{d}$. As a result, we have

$$\epsilon = 2 \frac{d}{\sqrt{D}} \sqrt{\ln\left(\frac{1.25}{\delta}\right)}.$$

F Details of Experiments

We train our models based on the data-driven version of the CFUR formulation presented in Section 3 using TensorFlow [Abadi et al., 2016].

F.1 GENKI Dataset

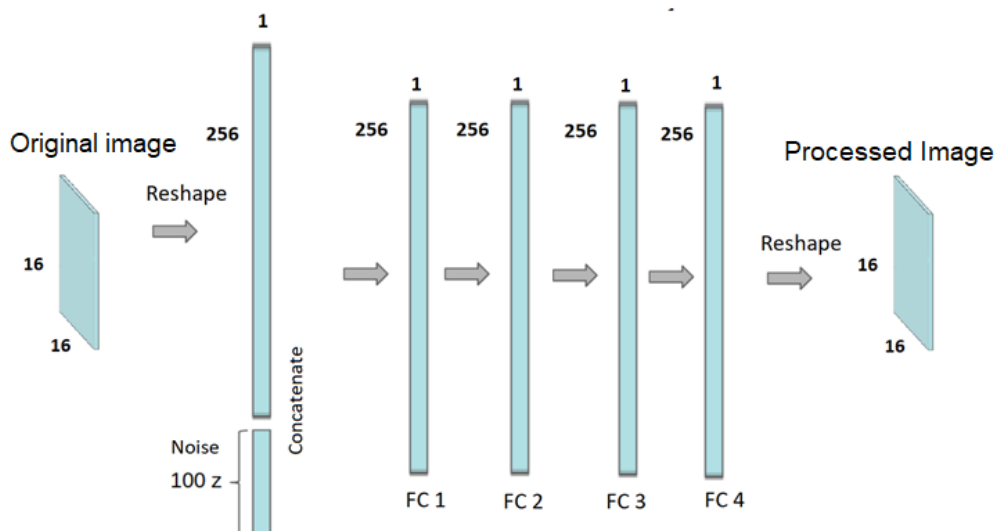


Figure 17: Feedforward neural network decorrelator for the GENKI dataset

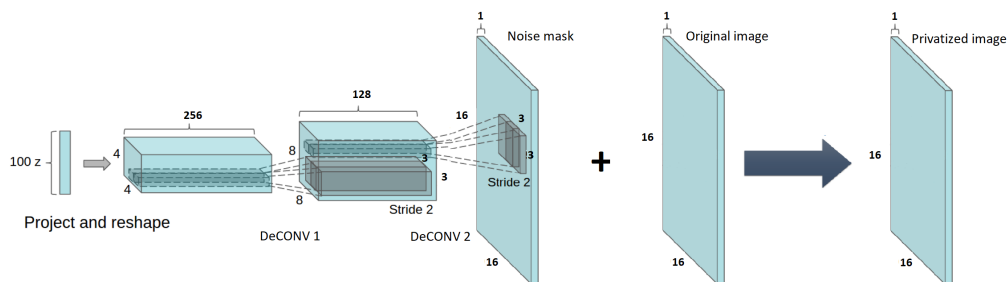


Figure 18: Transposed convolution neural network decorrelator for the GENKI dataset

ARCHITECTURE. The FNND is modeled by a four-layer feedforward neural network. We first reshape each image to a vector (256×1), and then concatenate it with a 100×1 Gaussian random noise vector. Each entry in the noise vector is sampled independently from a standard Gaussian distribution. We feed the entire vector to a four-layer fully connected (FC) neural network. Each layer has 256 neurons with a leaky ReLU activation function. Finally, we reshape the output of the last layer to a 16×16 image.

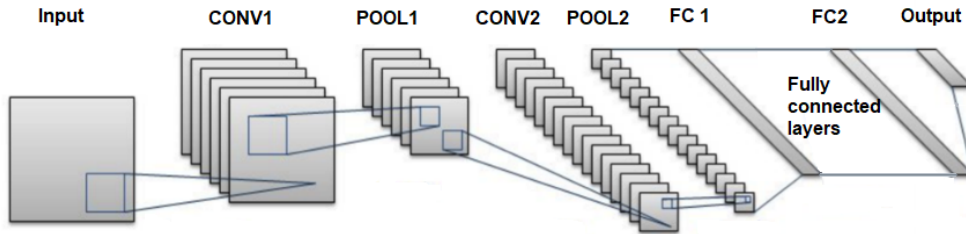


Figure 19: Convolutional neural network adversary for the GENKI dataset

To model the TCNND, we first generate a 100×1 Gaussian random vector and use a linear projection to map the noise vector to a $4 \times 4 \times 256$ feature tensor. The feature tensor is then fed to an initial transposed convolution layer (DeCONV) with 128 filters (filter size 3×3 , stride 2) and a ReLU activation, followed by another DeCONV layer with 1 filter (filter size 3×3 , stride 2) and a tanh activation. The output of the DeCONV layer is added to the original image to generate the processed data. For both decorrelators, we add batch normalization [Ioffe and Szegedy, 2015] on each hidden layer to prevent covariance shift and help gradients to flow. We model the adversary using convolutional neural networks (CNNs). This architecture outperforms most of other models for image classification [Krizhevsky et al., 2012, Szegedy et al., 2015].

Figure 19 illustrates the architecture of the adversary. The processed images are fed to two convolution layers (CONV) whose sizes are $3 \times 3 \times 32$ and $3 \times 3 \times 64$, respectively. Each convolution layer is followed by ReLU activation and batch normalization. The output of each convolution layer is fed to a 2×2 maxpool layer (POOL) to extract features for classification. The second maxpool layer is followed by two fully connected layers, each contains 1024 neurons with a batch normalization and a ReLU activation. Finally, the output of the last fully connected layer is mapped to the output layer, which contains two neurons capturing the belief of the subject being a male or a female.

F.2 HAR Dataset

ARCHITECTURE. We first concatenate the original data with a 100×1 Gaussian random noise vector. We then feed the entire 661×1 vector to a Feed Forward neural network with three hidden fully connected (FC) layers. Each hidden layer has 512 neurons with a leaky ReLU activation. Finally, we use another FC layer with 561 neurons to generate the processed data. For the adversary, we use a five-layer feedforward neural network. The hidden layers have 512, 512, 256, and 128 neurons with leaky ReLU activation, respectively. The output of the last hidden layer is mapped to the output layer, which contains 30 neurons capturing the belief of the subject’s identity. For both decorrelator and adversary, we add a batch normalization after the output of each hidden layer.

F.3 UCI Adult

Each sample in the UCI Adult dataset has both continuous and categorical features. Table 5 lists all the considered features. We perform a one hot encoding on each categorical feature in (S, X) and store the mapping function from the onehot encoding to the categorical data. For the continuous features in X , we restrict them into the interval $(0, 1)$ by normalization.

ARCHITECTURE. For the UCI Adult dataset, the two architectures used are shown in Fig. 20. We concatenate the pre-processed data with a same size standard Gaussian random vector, and feed the entire vector to the encoder. The encoder consists of two full-connected (FC) hidden layers

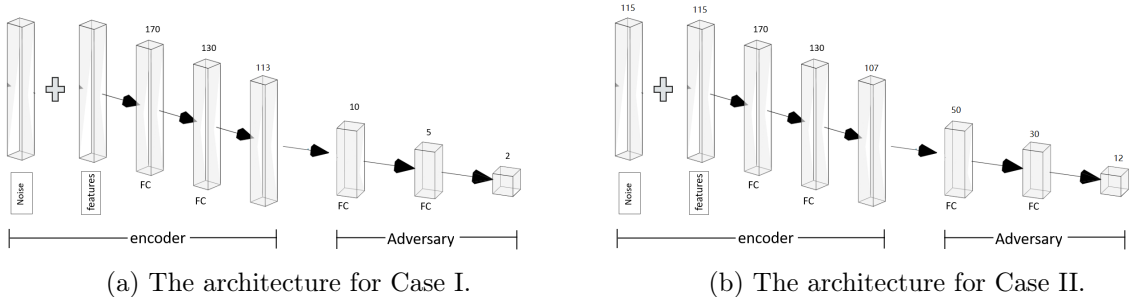


Figure 20: The architectures of the encoder and adversary for the UCI Adult dataset. Note that the appended noise has the same size of the input features and the output of the encoder has the same dimension as the feature variable X .

with the number of neurons as 170 and 130, respectively. Since the output representation X_r has the same dimension as the feature variable X , the output layer of the encoder has 113 (as shown in Fig. 20a) and 107 (as shown in Fig. 20b) neurons for Case I and Case II, respectively. We use a leaky Rectified linear unit (ReLU) activation function in the encoder. Finally, recall that we consider two cases for this dataset. Case I with binary (gender) sensitive feature and Case II with non-binary (gender and relationship) sensitive features. Furthermore, for Case I, the inputs can be either X only or both X and S . Therefore, in Fig. 20a, with only X as input to the encoder, the length of the input vector is 226 and when both X and S (binary) are inputs, the input length is 230. For both scenarios, the length of the encoder’s output is 113. In Fig. 20b, since the input is X and S , its input is 230; on the other hand, the length of the encoder’s output is 107 since S is non-binary in this case.

For Case I, the adversarial classifier in Fig. 20a consists of three full-connected (FC) layers with the number of neurons as 10, 5 as well as 2, respectively, and it takes X_r as the input and outputs a belief distribution for the binary sensitive variable S (i.e., gender). Here a ReLU is used as the activation function in the two hidden layers and the soft-max is used in the output layer to generate a belief distribution for gender. The same architecture is used for the downstream application of salary classification. For Case II, the adversarial classifier in Fig. 20b consists of three full-connected (FC) layers with the number of neurons as 50, 30 as well as 12, respectively. Here a Leaky ReLU is used as the activation function in the two hidden layers and the soft-max is used in the output layer. All of the above models use log-loss as the loss function and are optimized by a Adam optimizer.

F.4 UTKFace Dataset

We reshape 200×200 aligned-colorful faces in the UTKFace dataset consists into 64×64 colorful images.

ARCHITECTURE. For the UTKFace dataset, the used architectures are shown in Figs. 21, 22 and 23. Fig. 21 gives the architecture of the CFUR model which consists of an encoder and an adversarial classifier. The encoder is implemented by a noisy auto-encoder whose encoder transforms the original 64×64 RGB-images to a 4096-dimensional feature vector. Different from standard auto-encoder, which directly feeds the feature vector into the encoder part. Here, the feature vector is mixed with a 4096-dimensional standard normal random vector¹⁰, and then, fed into a decoder to reconstruct a 64×64 colorful image, which is the universal representation X_r . Specifically, the encoder part of the autoencoder consists of 4 convolution layers with 128, 64, 64 and 64 output

¹⁰A random vector is a standard normal random vector if all of its components are independent and identically following the standard normal distribution.

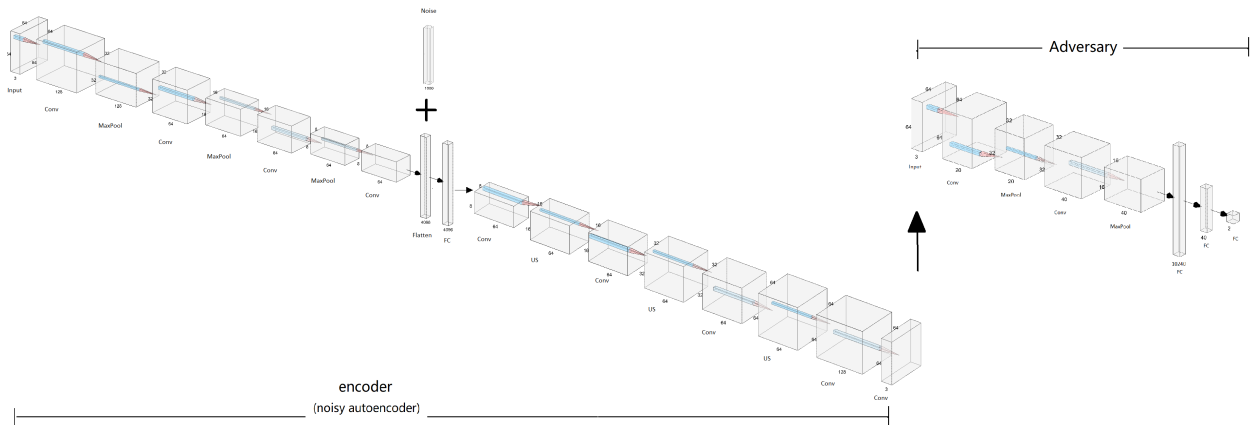


Figure 21: The architectures of the encoder and adversary for the UTKFace dataset

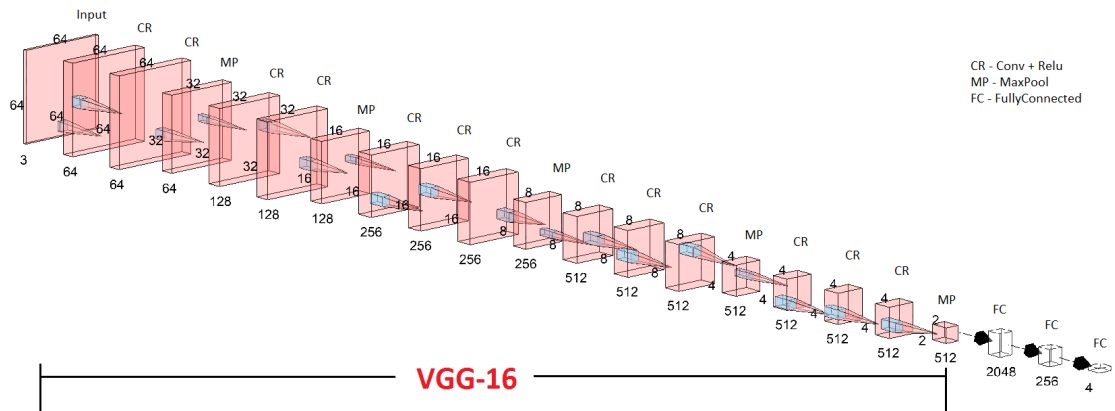


Figure 22: The architecture of the neural network for ethnicity classification for the UTKFace dataset.

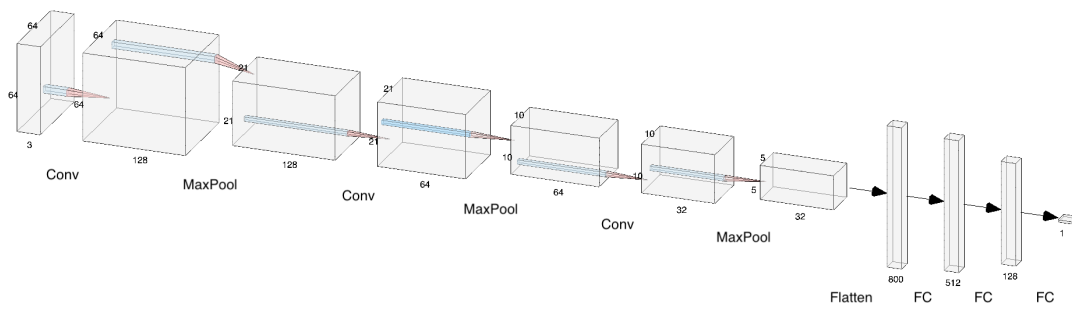


Figure 23: The architecture of the neural network for age regression for the UTKFace dataset.

channels, respectively, and 3×2 -max pooling layers following the first 3 convolution layers. The encoder part is followed by 2 fully-connected layers with 4096 neurons which mixes the noise and the output feature vector. The following decoder part consists of 5 convolution layers with 64, 64, 64, 128 and 3 output channels, respectively, and 3×2 -up-sampling layers following the first 3 convolution layers. The adversarial classifier takes into the representation X_r and outputs the prediction of the sensitive information gender. It consists of 2 convolution layers with 20 and 40 output channels, respectively, 2×2 -max pooling layers following each of the convolution layers and 2 full-connected layers with 40 and 2 neurons, respectively. The size of kernels in convolution layers is 3×3 . All convolution and full-connected layers use ReLU as the activation function except the last layers of the decoder and the adversarial which use sigmoid and softmax, respectively. The encoder and adversarial classifier use the square-loss and log-loss as the loss functions, respectively, and both of them are optimized by Adam Optimizer.

Fig. 22 gives the architecture of the downstream non-binary classification for ethnicity. The classifier is built by changing the top (last) 3 fully-connected layers of the VGG 16 model¹¹ pre-trained on ImageNet. The first one layer has 256 neurons with ReLU as the activation function and is followed by a Dropout layer with the rate 0.5, and the second one has 4 neurons with softmax as the activation function. The classifier use log-loss and is optimized by a Stochastic Gradient Descent Optimizer. Fig. 23 shows the architecture for the the downstream application of age regression. The regressor consists of three 3×3 convolution layers with 128, 64 and 32 output channels, three 2×2 -max pooling layers following each of the convolution layers, and three fully-connected layers with 512, 128 and 1 neurons, respectively. All layers use ReLU as the activation function except the last layer which uses a linear activation. The model uses the squared loss as the loss function and is optimized by a Adam Optimizer.

References

- Martín Abadi and David G Andersen. Learning to protect communications with adversarial neural cryptography. *arXiv preprint arXiv:1610.06918*, 2016.
- Martín Abadi, Ashish Agarwal, Paul Barham, Eugene Brevdo, Zhifeng Chen, Craig Citro, Greg S Corrado, Andy Davis, Jeffrey Dean, Matthieu Devin, et al. Tensorflow: Large-scale machine learning on heterogeneous distributed systems. *arXiv preprint arXiv:1603.04467*, 2016.
- Alekh Agarwal, Miroslav Dudik, and Zhiwei Steven Wu. Fair regression: Quantitative definitions and reduction-based algorithms. In *International Conference on Machine Learning*, pages 120–129, 2019.
- Alexander A Alemi, Ian Fischer, Joshua V Dillon, and Kevin Murphy. Deep variational information bottleneck. *arXiv preprint arXiv:1612.00410*, 2016.
- Davide Anguita, Alessandro Ghio, Luca Oneto, Xavier Parra, and Jorge Luis Reyes-Ortiz. A public domain dataset for human activity recognition using smartphones. In *ESANN*, 2013.
- Shahab Asoodeh, Mario Diaz, Fady Alajaji, and Tamás Linder. Estimation efficiency under privacy constraints. *IEEE Transactions on Information Theory*, 65(3):1512–1534, 2018.
- Solon Barocas and Andrew D Selbst. Big data’s disparate impact. *Calif. L. Rev.*, 104:671, 2016.

¹¹<https://keras.io/applications/#vgg16>

- Martin Bertran, Natalia Martinez, Afroditi Papadaki, Qiang Qiu, Miguel Rodrigues, Galen Reeves, and Guillermo Sapiro. Adversarially learned representations for information obfuscation and inference. In *International Conference on Machine Learning*, pages 614–623, 2019.
- Alex Beutel, Jilin Chen, Zhe Zhao, and Ed H Chi. Data decisions and theoretical implications when adversarially learning fair representations. *arXiv preprint arXiv:1707.00075*, 2017.
- Alex Beutel, Jilin Chen, Tulsee Doshi, Hai Qian, Li Wei, Yi Wu, Lukasz Heldt, Zhe Zhao, Lichan Hong, Ed H Chi, et al. Fairness in recommendation ranking through pairwise comparisons. In *Proceedings of the 25th ACM SIGKDD International Conference on Knowledge Discovery & Data Mining*, pages 2212–2220, 2019a.
- Alex Beutel, Jilin Chen, Tulsee Doshi, Hai Qian, Allison Woodruff, Christine Luu, Pierre Kreitmann, Jonathan Bischof, and Ed H Chi. Putting fairness principles into practice: Challenges, metrics, and improvements. In *Proceedings of the 2019 AAAI/ACM Conference on AI, Ethics, and Society*, pages 453–459, 2019b.
- Asia J Biega, Krishna P Gummadi, and Gerhard Weikum. Equity of attention: Amortizing individual fairness in rankings. In *The 41st international acm sigir conference on research & development in information retrieval*, pages 405–414, 2018.
- Toon Calders and Indrė Žliobaitė. Why unbiased computational processes can lead to discriminative decision procedures. In *Discrimination and privacy in the information society*, pages 43–57. Springer, 2013.
- F. P. Calmon and N. Fawaz. Privacy against statistical inference. In *Communication, Control, and Computing (Allerton), 2012 50th Annual Allerton Conference on*, pages 1401–1408, 2012.
- Flavio Calmon, Dennis Wei, Bhanukiran Vinzamuri, Karthikeyan Natesan Ramamurthy, and Kush R Varshney. Optimized pre-processing for discrimination prevention. In *Advances in Neural Information Processing Systems*, pages 3992–4001, 2017.
- Flavio Calmon, Dennis Wei, Bhanukiran Vinzamuri, Karthikeyan Natesan Ramamurthy, and Kush R Varshney. Data pre-processing for discrimination prevention: Information-theoretic optimization and analysis. *IEEE Journal of Selected Topics in Signal Processing*, 12(5):1106–1119, 2018.
- Alexandra Chouldechova. Fair prediction with disparate impact: A study of bias in recidivism prediction instruments. *Big data*, 5(2):153–163, 2017.
- Maximin Coavoux, Shashi Narayan, and Shay B Cohen. Privacy-preserving neural representations of text. In *Proceedings of the 2018 Conference on Empirical Methods in Natural Language Processing*, pages 1–10, 2018.
- Sam Corbett-Davies and Sharad Goel. The measure and mismeasure of fairness: A critical review of fair machine learning. *ArXiv*, abs/1808.00023, 2018.
- Andrew Cotter, Heinrich Jiang, Maya Gupta, Serena Wang, Taman Narayan, Seungil You, and Karthik Sridharan. Optimization with non-differentiable constraints with applications to fairness, recall, churn, and other goals. *Journal of Machine Learning Research*, 20(172):1–59, 2019a.
- Andrew Cotter, Heinrich Jiang, and Karthik Sridharan. Two-player games for efficient non-convex constrained optimization. In *Proceedings of the 30th International Conference on Algorithmic Learning Theory*, volume 98 of *Proceedings of Machine Learning Research*, pages 300–332, Chicago, Illinois, 22–24 Mar 2019b. PMLR.

- Elliot Creager, David Madras, Joern-Henrik Jacobsen, Marissa Weis, Kevin Swersky, Toniann Pitassi, and Richard Zemel. Flexibly fair representation learning by disentanglement. In *Proceedings of the 36th International Conference on Machine Learning*, volume 97 of *Proceedings of Machine Learning Research*, pages 1436–1445, Long Beach, California, USA, 09–15 Jun 2019.
- John Duchi, Michael Jordan, and Martin Wainwright. Local privacy and statistical minimax rates. In *Foundations of Computer Science (FOCS), 2013 IEEE 54th Annual Symposium on*, pages 429–438. IEEE, 2013.
- Cynthia Dwork, Moritz Hardt, Toniann Pitassi, Omer Reingold, and Richard Zemel. Fairness through awareness. In *Proceedings of the 3rd innovations in theoretical computer science conference*, pages 214–226. ACM, 2012.
- Jonathan Eckstein and W Yao. Augmented lagrangian and alternating direction methods for convex optimization: A tutorial and some illustrative computational results. *RUTCOR Research Reports*, 32, 2012.
- Harrison Edwards and Amos J. Storkey. Censoring representations with an adversary. In *The 4th International Conference on Learning Representations, ICLR*, 2016.
- Yanai Elazar and Yoav Goldberg. Adversarial removal of demographic attributes from text data. In *Proceedings of the 2018 Conference on Empirical Methods in Natural Language Processing*, pages 11–21, 2018.
- Michael Feldman, Sorelle A Friedler, John Moeller, Carlos Scheidegger, and Suresh Venkatasubramanian. Certifying and removing disparate impact. In *proceedings of the 21th ACM SIGKDD international conference on knowledge discovery and data mining*, pages 259–268, 2015a.
- Michael Feldman, Sorelle A Friedler, John Moeller, Carlos Scheidegger, and Suresh Venkatasubramanian. Certifying and removing disparate impact. In *Proceedings of the 21th ACM SIGKDD International Conference on Knowledge Discovery and Data Mining*, pages 259–268. ACM, 2015b.
- Benjamin Fish, Jeremy Kun, and Ádám D Lelkes. A confidence-based approach for balancing fairness and accuracy. In *Proceedings of the 2016 SIAM International Conference on Data Mining*, pages 144–152. SIAM, 2016.
- Robert G Gallager. *Stochastic processes: theory for applications*. Cambridge University Press, 2013.
- Yaroslav Ganin, Evgeniya Ustinova, Hana Ajakan, Pascal Germain, Hugo Larochelle, François Laviolette, Mario Marchand, and Victor Lempitsky. Domain-adversarial training of neural networks. *The Journal of Machine Learning Research*, 17(1):2096–2030, 2016.
- Sahaj Garg, Vincent Perot, Nicole Limtiaco, Ankur Taly, Ed H Chi, and Alex Beutel. Counterfactual fairness in text classification through robustness. In *Proceedings of the 2019 AAAI/ACM Conference on AI, Ethics, and Society*, pages 219–226, 2019.
- AmirEmad Ghassami, Sajad Khodadadian, and Negar Kiyavash. Fairness in supervised learning: An information theoretic approach. *arXiv preprint arXiv:1801.04378*, 2018.
- Ian Goodfellow, Jean Pouget-Abadie, Mehdi Mirza, Bing Xu, David Warde-Farley, Sherjil Ozair, Aaron Courville, and Yoshua Bengio. Generative adversarial nets. In *Advances in neural information processing systems*, pages 2672–2680, 2014.

- Google. Tensorflow constrained optimization (TFCO). https://github.com/google-research/tensorflow_constrained_optimization/blob/master/README.md.
- Maya Gupta, Andrew Cotter, Mahdi Milani Fard, and Serena Wang. Proxy fairness. *arXiv:1806.11212*, 2018.
- Michael Gutmann and Aapo Hyvärinen. Noise-contrastive estimation: A new estimation principle for unnormalized statistical models. In *Proceedings of the Thirteenth International Conference on Artificial Intelligence and Statistics*, pages 297–304, 2010.
- Sara Hajian, Josep Domingo-Ferrer, Anna Monreale, Dino Pedreschi, and Fosca Giannotti. Discrimination-and privacy-aware patterns. *Data Mining and Knowledge Discovery*, 29(6):1733–1782, 2015.
- Jihun Hamm. Minimax filter: learning to preserve privacy from inference attacks. *The Journal of Machine Learning Research*, 18(1):4704–4734, 2017.
- Moritz Hardt, Eric Price, and Nati Srebro. Equality of opportunity in supervised learning. In *Advances in neural information processing systems*, pages 3315–3323, 2016.
- Chong Huang, Peter Kairouz, Xiao Chen, Lalitha Sankar, and Ram Rajagopal. Context-aware generative adversarial privacy. *Entropy*, 19(12):656, 2017.
- Sergey Ioffe and Christian Szegedy. Batch normalization: Accelerating deep network training by reducing internal covariate shift. *arXiv preprint arXiv:1502.03167*, 2015.
- Yusuke Iwasawa, Kotaro Nakayama, Ikuko Eguchi Yairi, and Yutaka Matsuo. Privacy issues regarding the application of dnns to activity-recognition using wearables and its countermeasures by use of adversarial training. In *Proceedings of the 26th International Joint Conference on Artificial Intelligence*, pages 1930–1936. AAAI Press, 2017.
- Christopher Jung, Michael Kearns, Seth Neel, Aaron Roth, Logan Stapleton, and Zhiwei Steven Wu. Eliciting and enforcing subjective individual fairness. *arXiv:1905.10660*, 2019.
- Peter Kairouz, Jiachun Liao, Chong Huang, and Lalitha Sankar. Censored and fair universal representations using generative adversarial models. https://github.com/LalithaSankarResearch/CFUR_source-code.
- Peter Kairouz, Sewoong Oh, and Pramod Viswanath. Extremal mechanisms for local differential privacy. *J. Mach. Learn. Res.*, 17(1):492–542, January 2016. ISSN 1532-4435. URL <http://dl.acm.org/citation.cfm?id=2946645.2946662>.
- Michael Kearns, Seth Neel, Aaron Roth, and Zhiwei Steven Wu. Preventing fairness gerrymandering: Auditing and learning for subgroup fairness. In *International Conference on Machine Learning*, pages 2564–2572, 2018.
- Ron Kohavi. Scaling up the accuracy of naive-bayes classifiers: A decision-tree hybrid. In *Kdd*, volume 96, pages 202–207, 1996.
- Alexander Kraskov, Harald Stögbauer, and Peter Grassberger. Estimating mutual information. *Physical review E*, 69(6):066138, 2004.
- Alex Krizhevsky, Ilya Sutskever, and Geoffrey E Hinton. Imagenet classification with deep convolutional neural networks. In *Advances in neural information processing systems*, pages 1097–1105, 2012.

- Helen F Ladd. Evidence on discrimination in mortgage lending. *Journal of Economic Perspectives*, 12(2):41–62, 1998.
- Preethi Lahoti, Krishna P Gummadi, and Gerhard Weikum. ifair: Learning individually fair data representations for algorithmic decision making. In *2019 IEEE 35th International Conference on Data Engineering (ICDE)*, pages 1334–1345. IEEE, 2019.
- Dirk Lewandowski and Ulrike Spree. Ranking of wikipedia articles in search engines revisited: Fair ranking for reasonable quality? *Journal of the American Society for Information Science and technology*, 62(1):117–132, 2011.
- Yitong Li, Timothy Baldwin, and Trevor Cohn. Towards robust and privacy-preserving text representations. In *Proceedings of the 56th Annual Meeting of the Association for Computational Linguistics (Volume 2: Short Papers)*, pages 25–30, 2018.
- Jiachun Liao, Oliver Kosut, Lalitha Sankar, and Flavio P Calmon. Privacy under hard distortion constraints. *arXiv preprint arXiv:1806.00063*, 2018.
- Walter E Lillo, Mei Heng Loh, Stefen Hui, and Stanislaw H Zak. On solving constrained optimization problems with neural networks: A penalty method approach. *IEEE Transactions on neural networks*, 4(6):931–940, 1993.
- C Louizos, K Swersky, Y Li, M Welling, and R Zemel. The variational fair autoencoder. 2016.
- Pauline Luc, Camille Couprie, Soumith Chintala, and Jakob Verbeek. Semantic segmentation using adversarial networks. *arXiv:1611.08408*, 2016.
- David Madras, Elliot Creager, Toniann Pitassi, and Richard Zemel. Learning adversarially fair and transferable representations. *arXiv:1802.06309*, 2018.
- Daniel McNamara, Cheng Soon Ong, and Robert C Williamson. Provably fair representations. *arXiv:1710.04394*, 2017.
- Ninareh Mehrabi, Fred Morstatter, Nripsuta Saxena, Kristina Lerman, and Aram Galstyan. A survey on bias and fairness in machine learning. *ArXiv*, abs/1908.09635, 2019.
- Mehdi Mirza and Simon Osindero. Conditional generative adversarial nets. *arXiv preprint arXiv:1411.1784*, 2014.
- Daniel Moyer, Shuyang Gao, Rob Brekelmans, Aram Galstyan, and Greg Ver Steeg. Invariant representations without adversarial training. In *Advances in Neural Information Processing Systems*, pages 9084–9093, 2018.
- Harikrishna Narasimhan, Andrew Cotter, Maya Gupta, and Serena Wang. Pairwise fairness for ranking and regression. *arXiv preprint arXiv:1906.05330*, 2019.
- Tan Nguyen and Scott Sanner. Algorithms for direct 0–1 loss optimization in binary classification. In *International Conference on Machine Learning*, pages 1085–1093, 2013.
- Augustus Odena. Semi-supervised learning with generative adversarial networks. *arXiv:1606.01583*, 2016.
- Dino Pedreshi, Salvatore Ruggieri, and Franco Turini. Discrimination-aware data mining. In *Proceedings of the 14th ACM SIGKDD international conference on Knowledge discovery and data mining*, pages 560–568. ACM, 2008.

- Nisarg Raval, Ashwin Machanavajjhala, and Landon P Cox. Protecting visual secrets using adversarial nets. In *CVPR Workshop Proceedings*, 2017.
- Tim Salimans, Ian Goodfellow, Wojciech Zaremba, Vicki Cheung, Alec Radford, and Xi Chen. Improved techniques for training gans. In *Advances in neural information processing systems*, pages 2234–2242, 2016.
- Ashudeep Singh and Thorsten Joachims. Fairness of exposure in rankings. In *Proceedings of the 24th ACM SIGKDD International Conference on Knowledge Discovery & Data Mining*, pages 2219–2228, 2018.
- Congzheng Song and Vitaly Shmatikov. Overlearning reveals sensitive attributes. *arXiv:1905.11742*, 2019.
- Christian Szegedy, Wei Liu, Yangqing Jia, Pierre Sermanet, Scott Reed, Dragomir Anguelov, Dumitru Erhan, Vincent Vanhoucke, Andrew Rabinovich, et al. Going deeper with convolutions. *Cvpr*, 2015.
- Ardhendu Tripathy, Ye Wang, and Prakash Ishwar. Privacy-preserving adversarial networks. *arXiv preprint arXiv:1712.07008*, 2017.
- Sergio Verdú. α -mutual information. In *2015 Information Theory and Applications Workshop (ITA)*, 2015.
- Jacob Whitehill and Javier Movellan. Discriminately decreasing discriminability with learned image filters. In *Computer Vision and Pattern Recognition (CVPR), 2012 IEEE Conference on*, pages 2488–2495. IEEE, 2012.
- Qizhe Xie, Zihang Dai, Yulun Du, Eduard Hovy, and Graham Neubig. Controllable invariance through adversarial feature learning. In *Advances in Neural Information Processing Systems*, pages 585–596, 2017.
- Ke Yang and Julia Stoyanovich. Measuring fairness in ranked outputs. In *Proceedings of the 29th International Conference on Scientific and Statistical Database Management*, pages 1–6, 2017.
- Meike Zehlike, Francesco Bonchi, Carlos Castillo, Sara Hajian, Mohamed Megahed, and Ricardo Baeza-Yates. Fa*ir: A fair top-k ranking algorithm. In *Proceedings of the 2017 ACM on Conference on Information and Knowledge Management*, pages 1569–1578, 2017.
- Brian Hu Zhang, Blake Lemoine, and Margaret Mitchell. Mitigating unwanted biases with adversarial learning. *arXiv preprint arXiv:1801.07593*, 2018.
- Song Yang Zhang, Zhifei and Hairong Qi. Age progression/regression by conditional adversarial autoencoder. In *IEEE Conference on Computer Vision and Pattern Recognition (CVPR)*. IEEE, 2017.